Electron-withdrawing groups as property tuners in functionalized terpyridine-based ligands in Eu(III) and Tb(III) complexes

Oksana Fizer,[1] Sina Chiniforoush,[2] Thomas Summers,[2] Mohammad Zafar Abbas,[1] David C. Cantu,[2] Ana de Bettencourt-Dias[1,*]

[1]Department of Chemistry, University of Nevada, Reno, NV 89557
[2]Department of Chemical and Material Engineering, University of Nevada, Reno, NV 89557
*abd@unr.edu

Table of Contents

NMR Spectroscopy

^{1}H-NMR

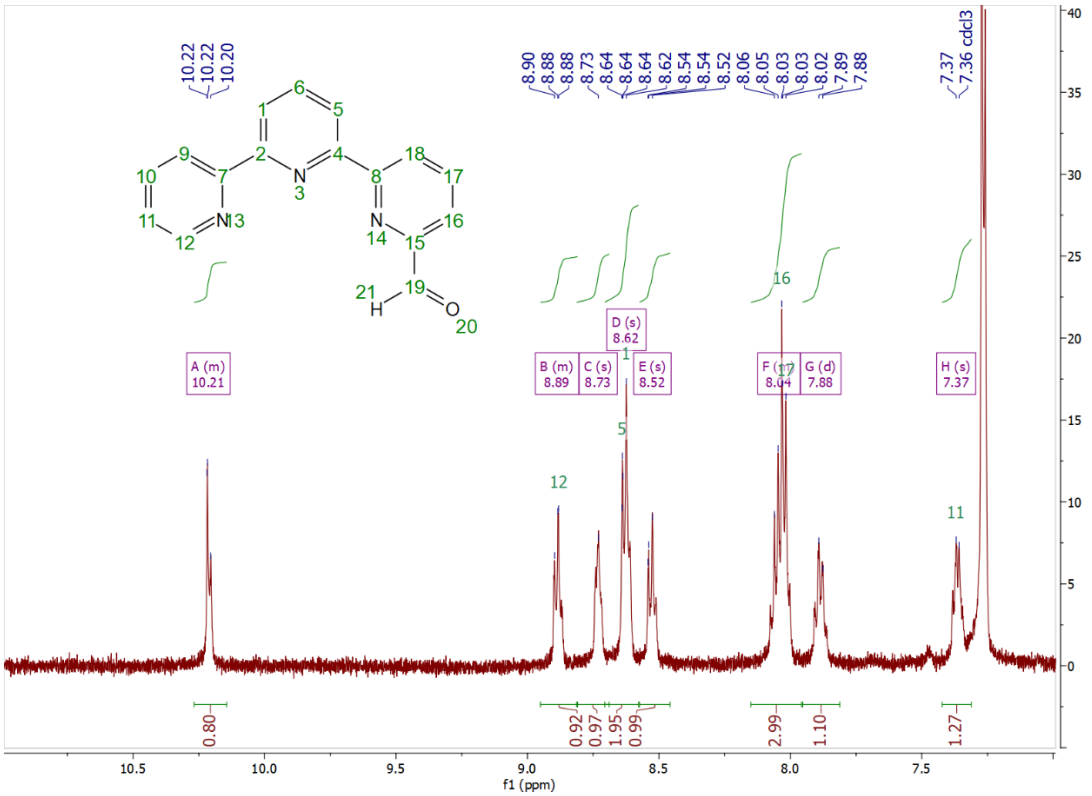

Fig. S1. ^{1}H-NMR spectrum of the terpyCHO in $CDCl_3$.

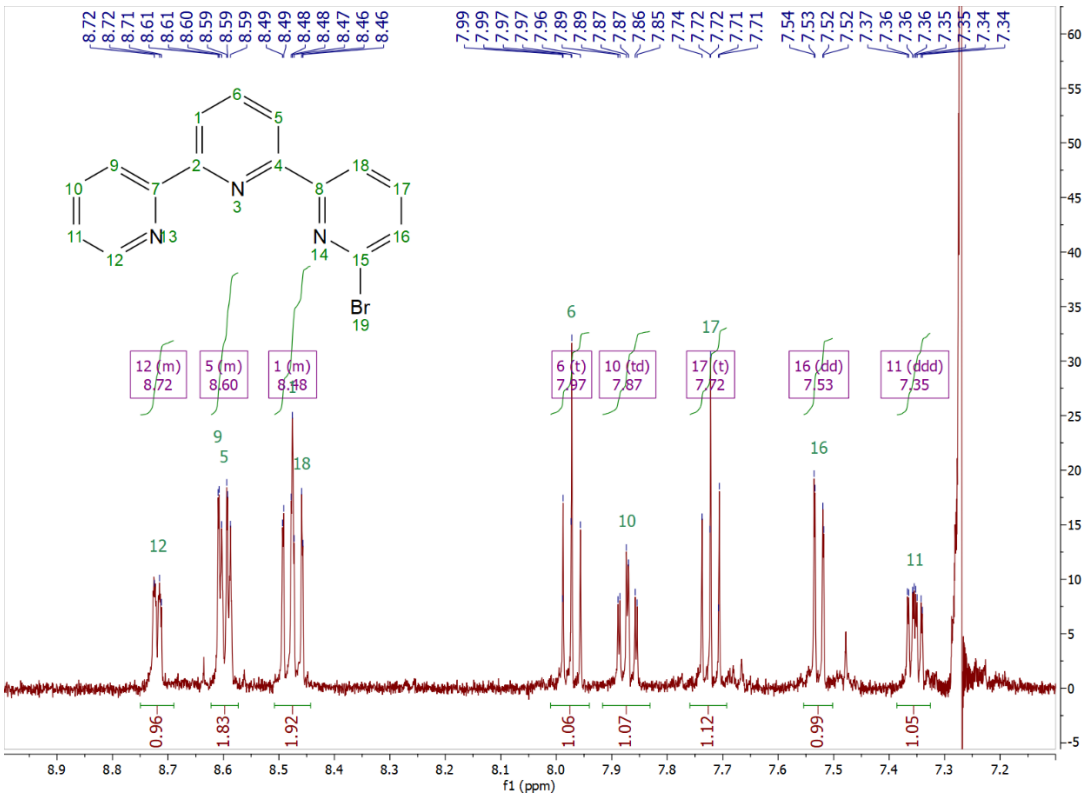

Fig. S2. ^{1}H-NMR spectrum of terpyBr in $CDCl_3$.

^{13}C-NMR

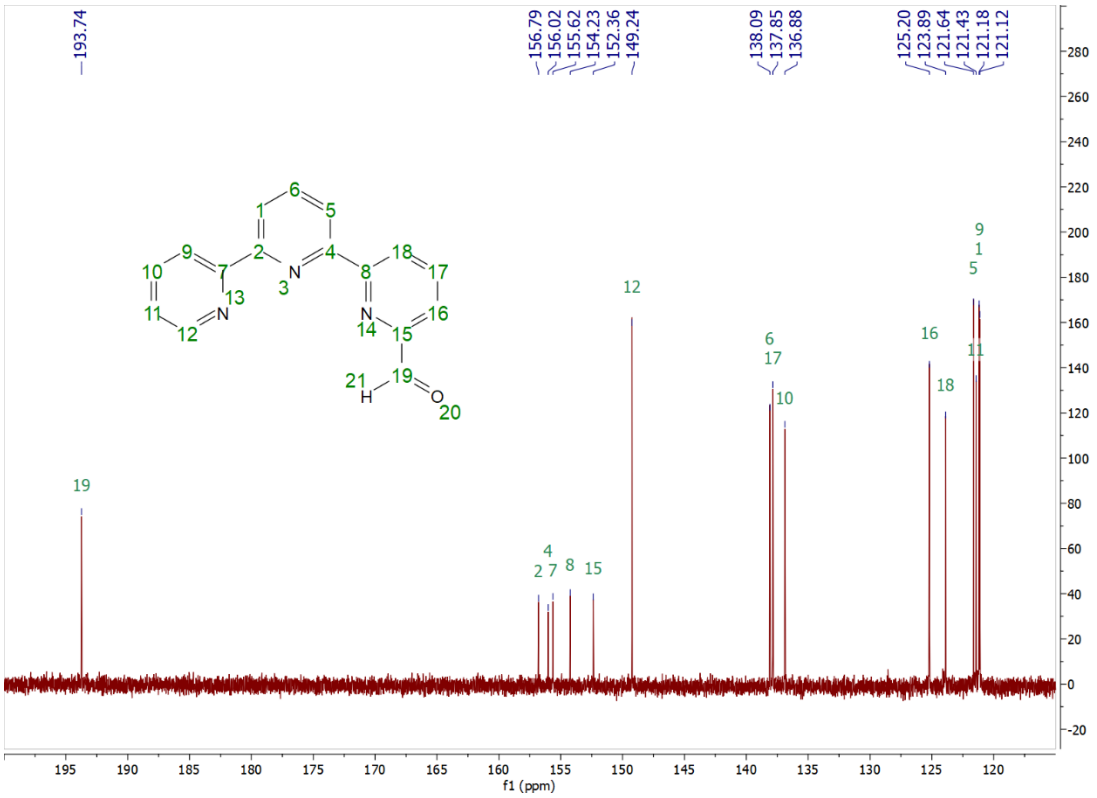

Fig. S3. ^{13}C-NMR spectrum of terpyCHO in $CDCl_3$.

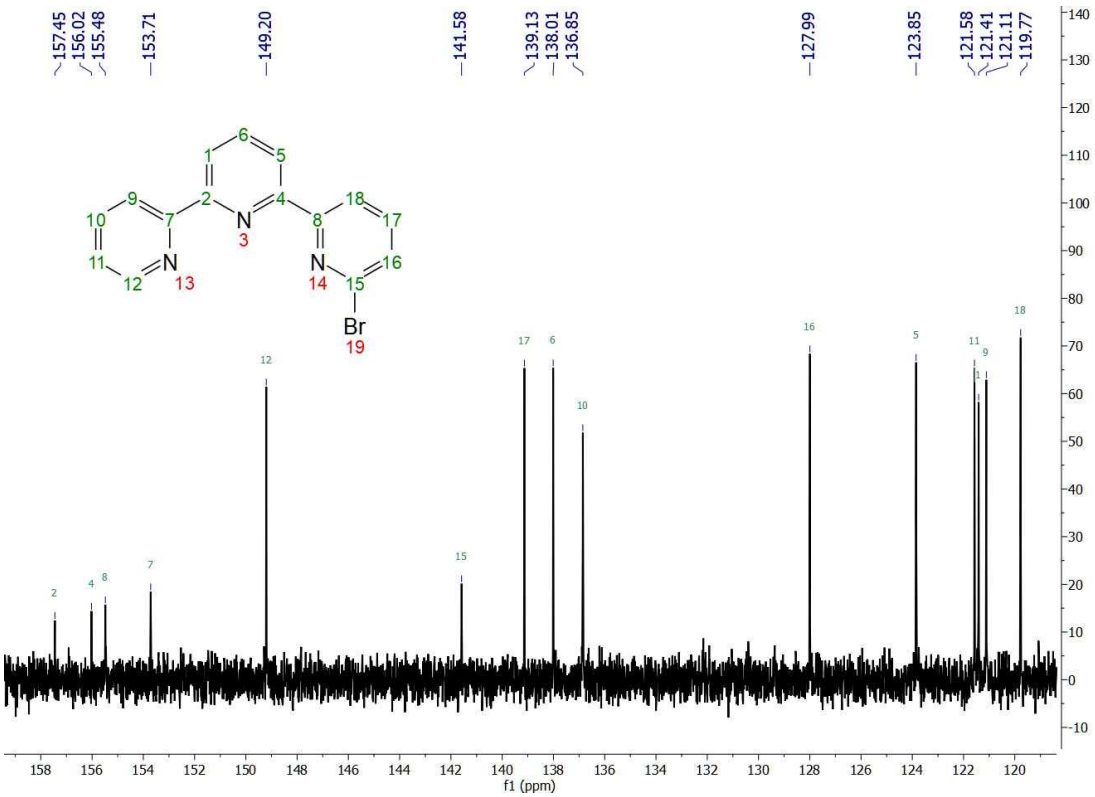

Fig. S4. ^{13}C-NMR spectrum of terpyBr in $CDCl_3$.

Mass Spectrometry

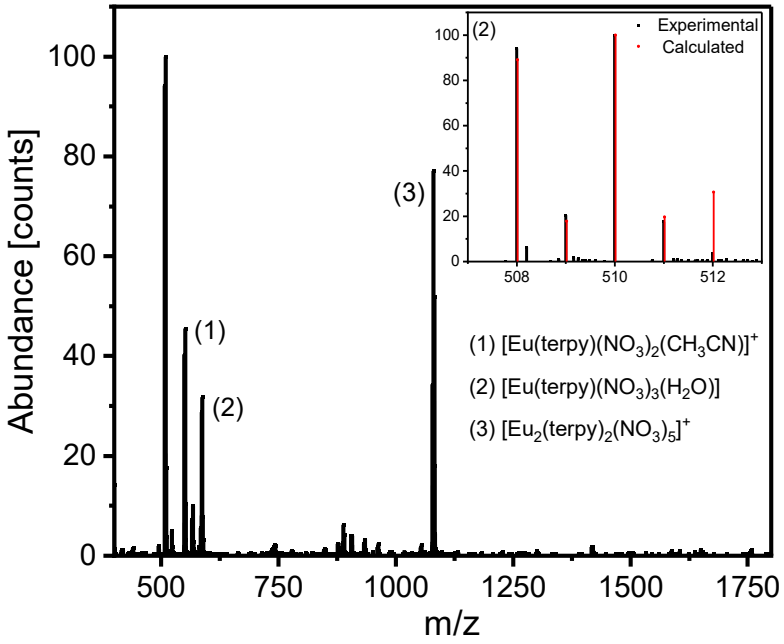

Fig. S5. Mass spectrum of [Eu(terpy)$(NO_3)_3$]. The inset shows the calculated and experimental isotope pattern.

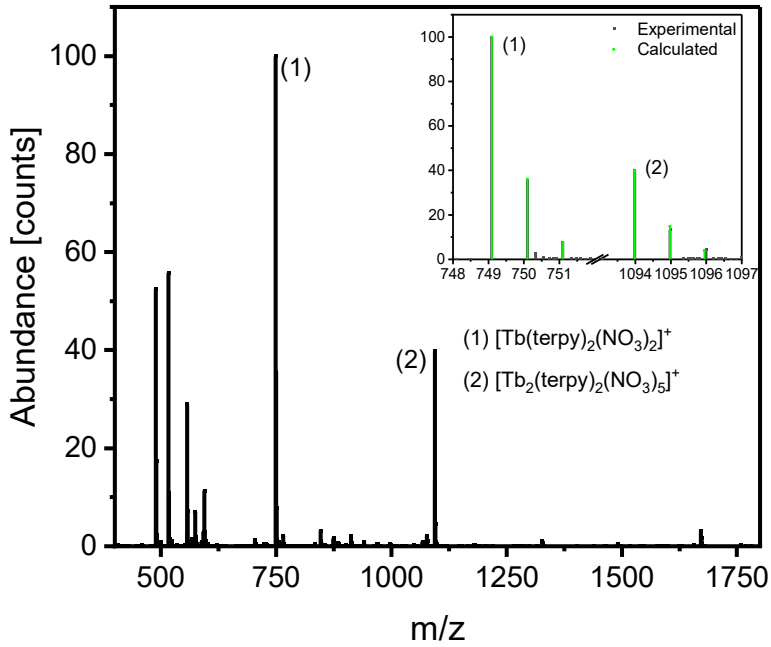

Fig. S6. Mass spectrum of [Tb(terpy)$(NO_3)_3$]. The inset shows the calculated and experimental isotope pattern.

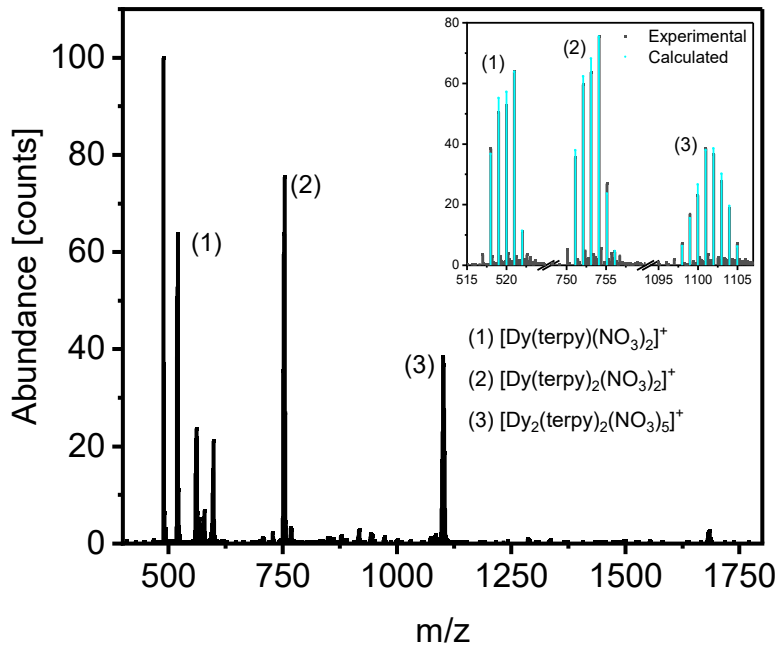

Fig. S7. Mass spectrum of [Dy-terpy$(NO_3)_3$]. The inset shows the calculated and experimental isotope pattern.

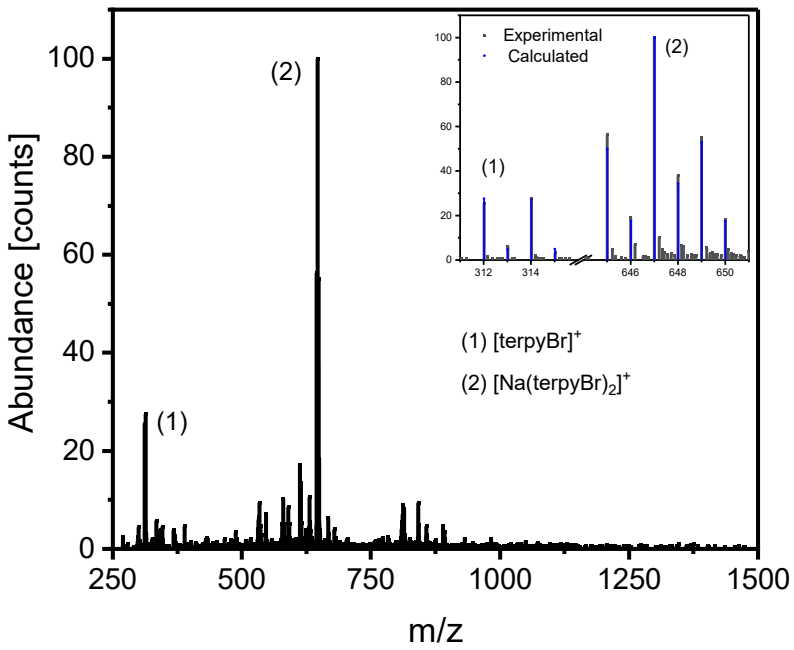

Fig. S8. Mass spectrum of terpyBr. The inset shows the calculated and experimental isotope pattern.

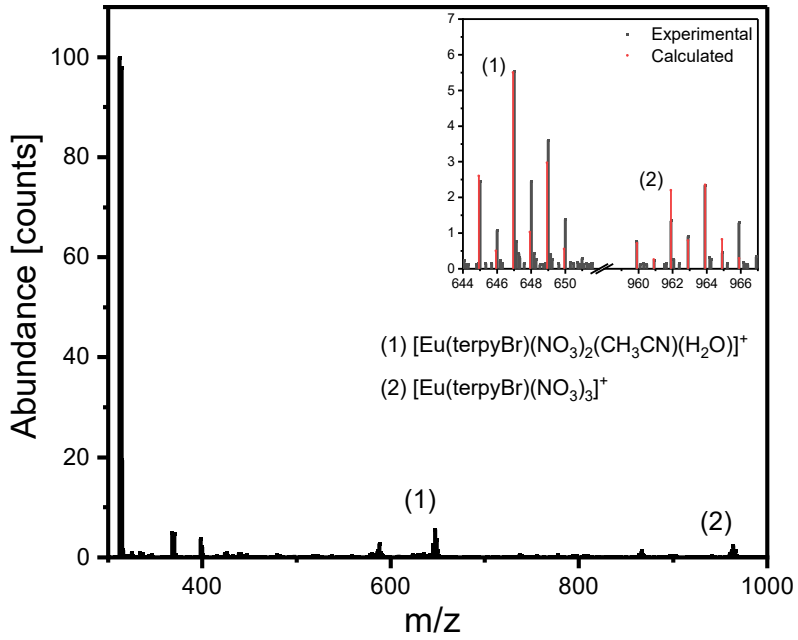

Fig. S9. Mass spectrum of [Eu(terpyBr)$(NO_3)_3$]. The inset shows the calculated and experimental isotope pattern.

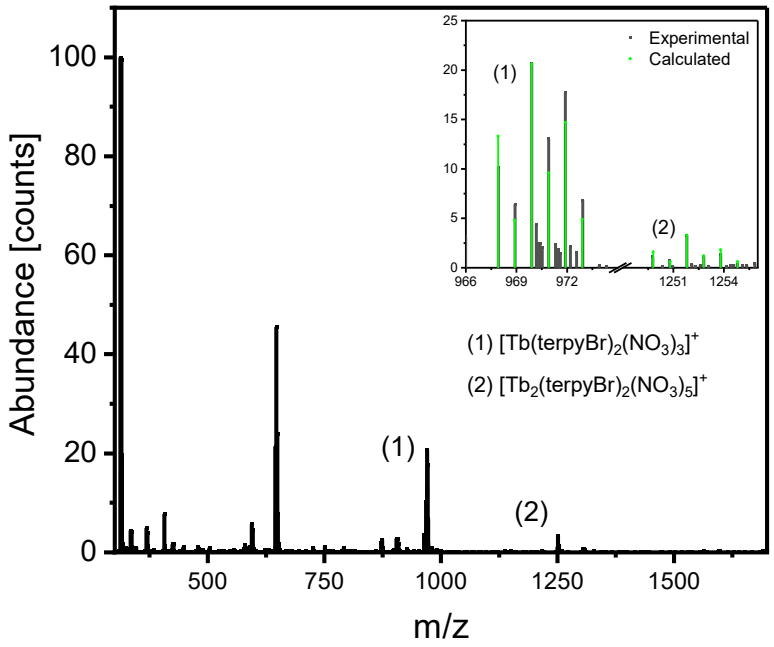

Fig. S10. Mass spectrum of [Tb(terpyBr)$(NO_3)_3$]. The inset shows the calculated and experimental isotope pattern.

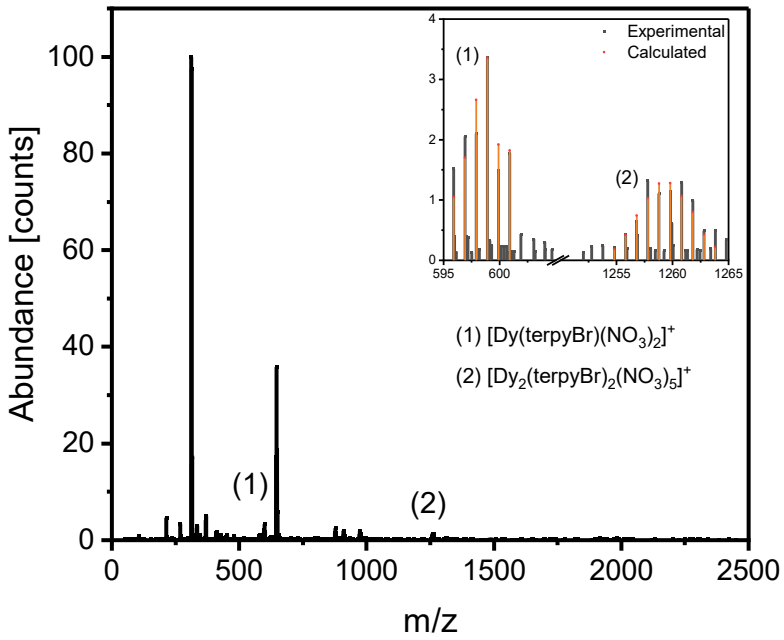

Fig. S11. Mass spectrum of [Dy(terpyBr)$(NO_3)_3$]. The inset shows the calculated and experimental isotope pattern.

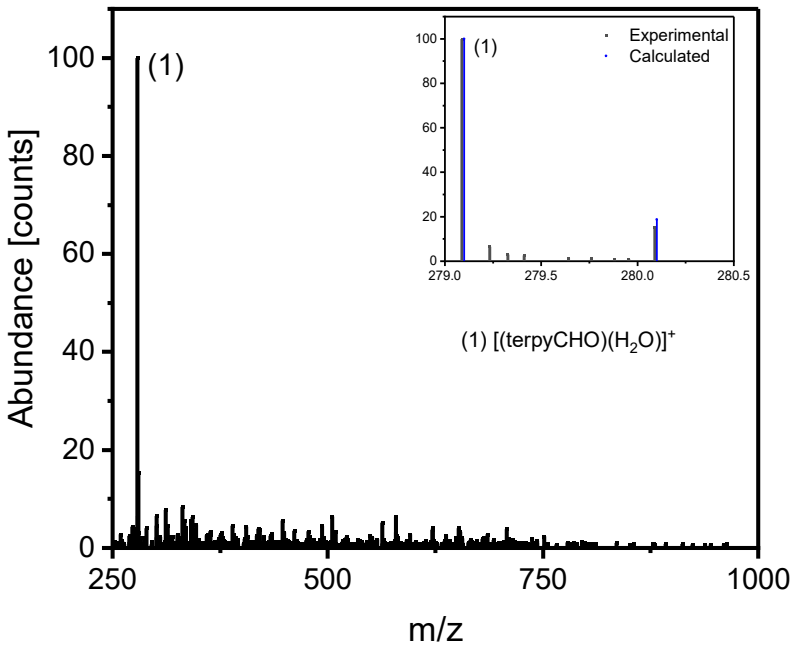

Fig. S12. Mass spectrum of terpyCHO. The inset shows the calculated and experimental isotope pattern.

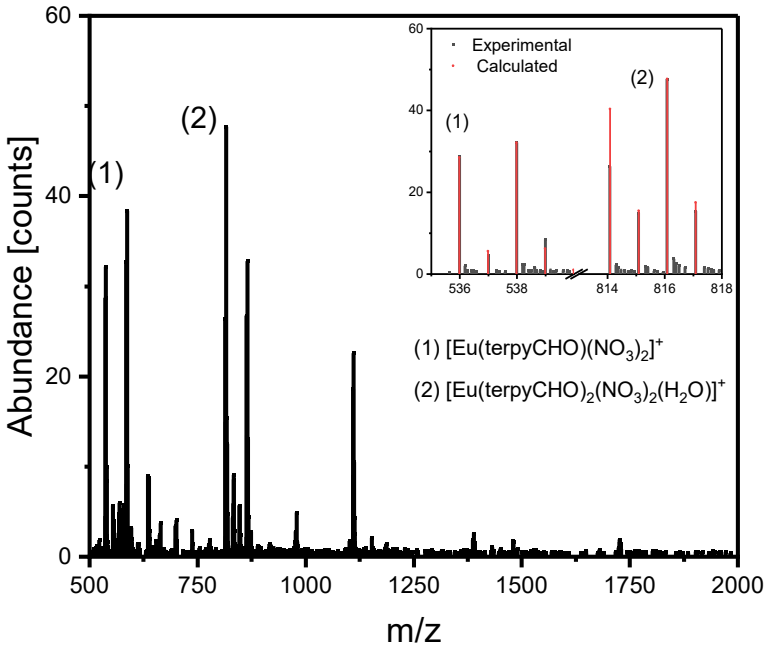

Fig. S13. Mass spectrum of [Eu(terpyCHO)(NO_3)$_3$]. The inset shows the calculated and experimental isotope pattern.

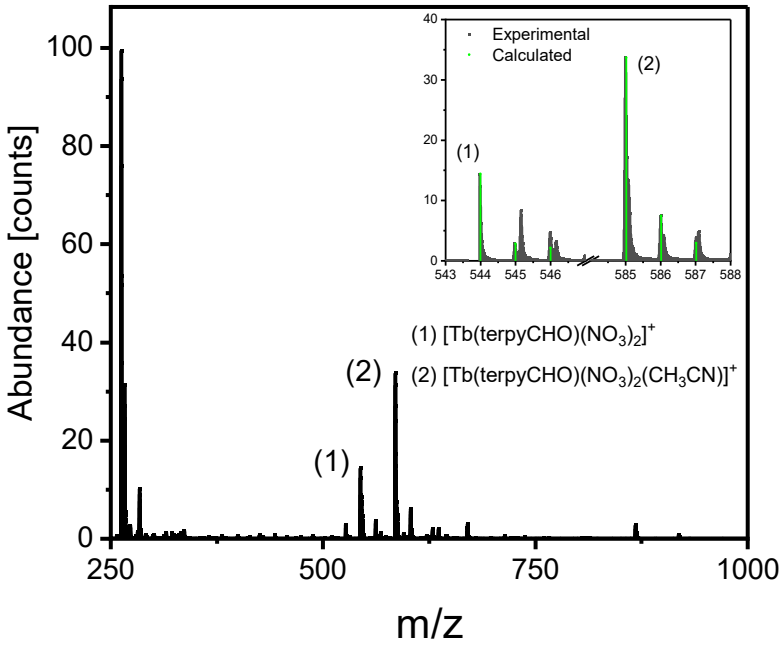

Fig. S14. Mass spectrum of [Tb(terpyCHO)(NO_3)$_3$]. The inset shows the calculated and experimental isotope pattern.

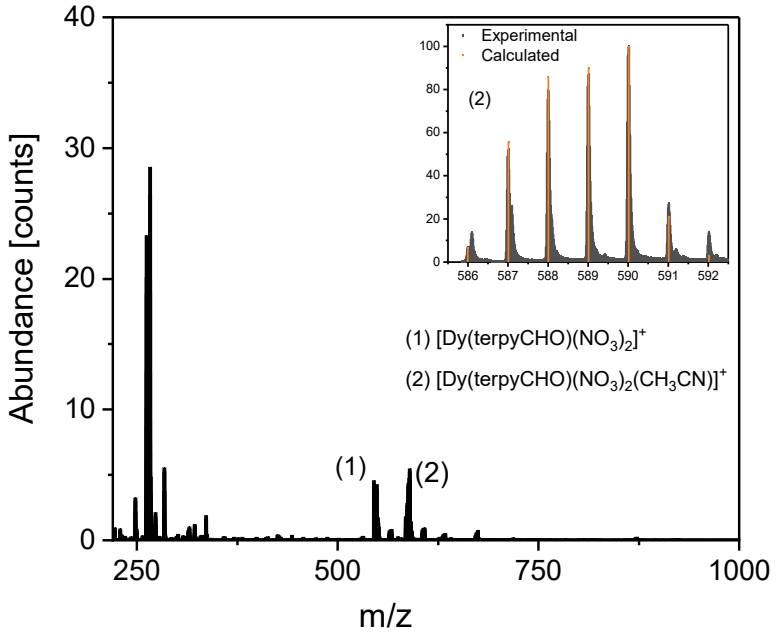

Fig. S15. Mass spectrum of [Dy(terpyCHO)(NO_3)$_3$]. The inset shows the calculated and experimental isotope pattern.

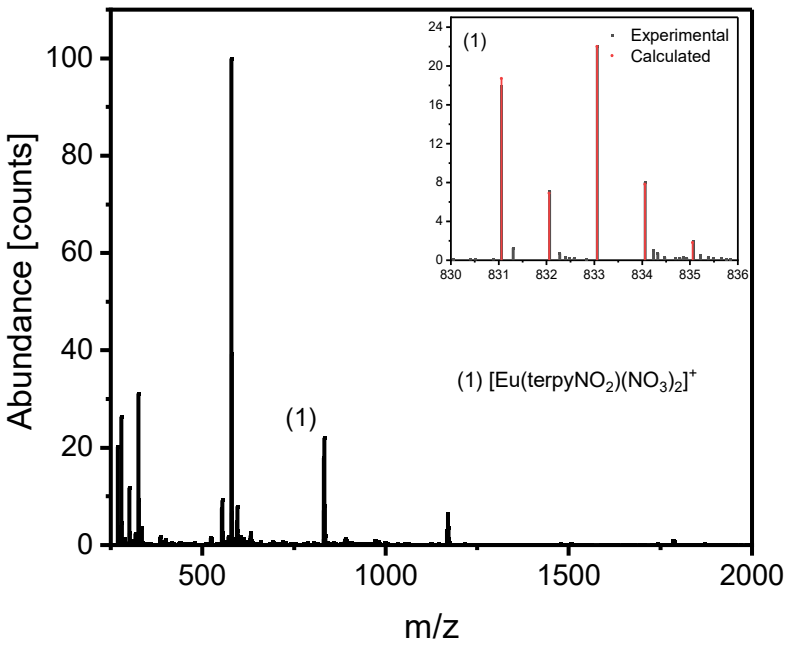

Fig. S16. Mass spectrum of [Eu(terpyNO_2)(NO_3)$_3$]. The inset shows the calculated and experimental isotope pattern.

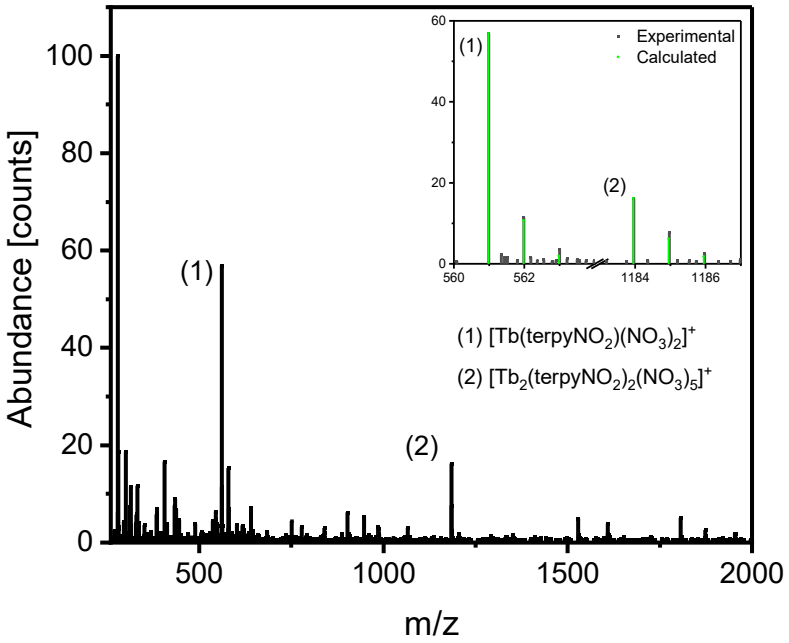

Fig. S17. Mass spectrum of [Tb(terpyNO$_2$)(NO$_3$)$_3$]. The inset shows the calculated and experimental isotope pattern.

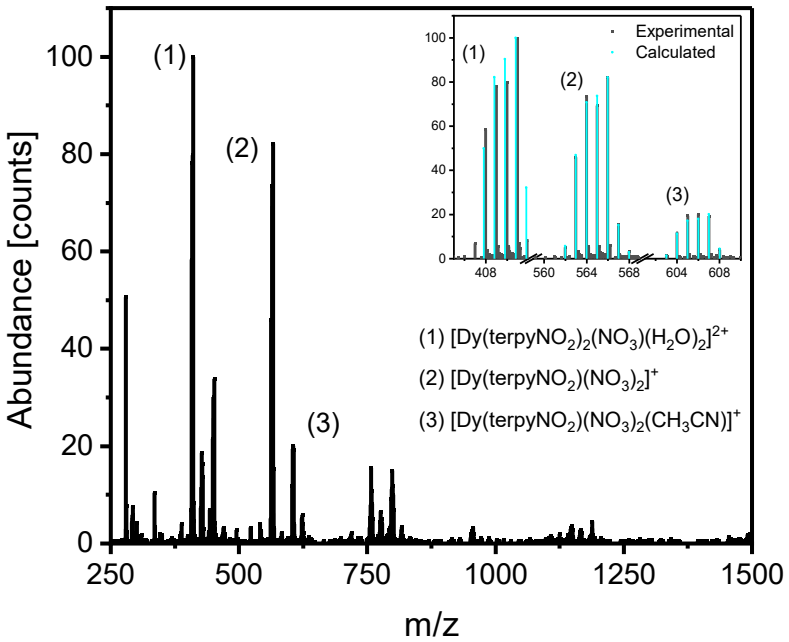

Fig. S18. Mass spectrum of [Dy(terpyNO$_2$)(NO$_3$)$_3$]. The inset shows the calculated and experimental isotope pattern.

Spectrophotometric Titrations

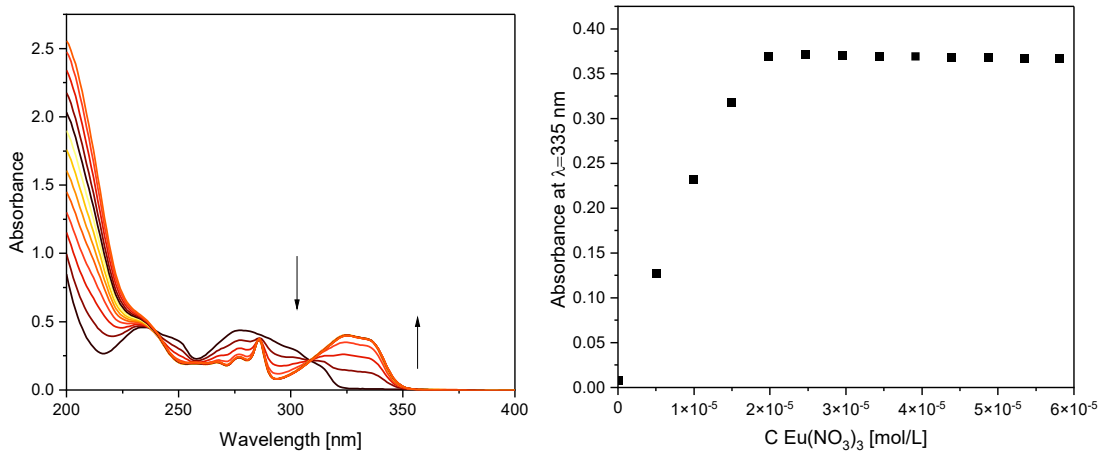

(a) **(b)**

Fig. S19. Spectrophotometric titration of 2×10^{-5} mol/L terpy with Eu(III) as the nitrate salt in MeCN at 298 K. **(a)** Absorption spectra and **(b)** absorbance at 335 nm with increasing Eu(III) concentration. Arrows indicate increasing and decreasing peaks.

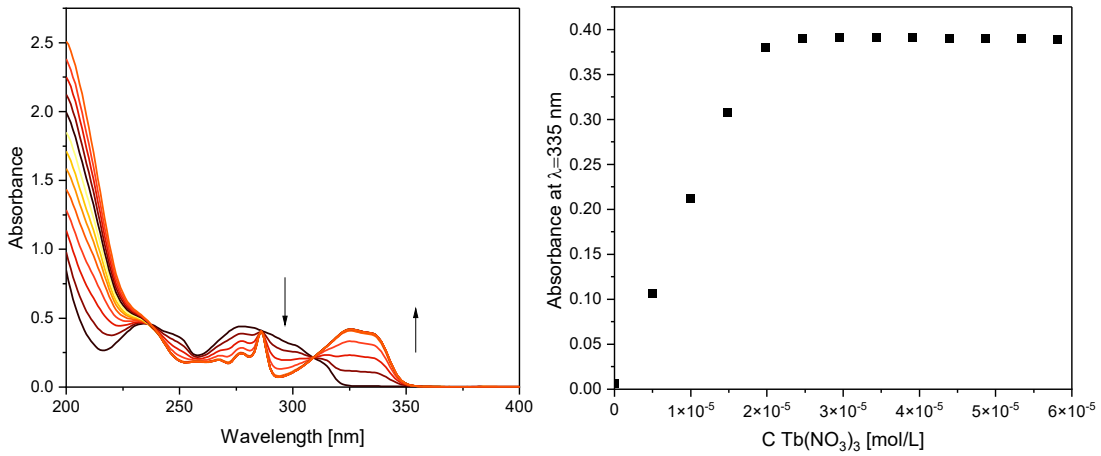

(a) **(b)**

Fig. S20. Spectrophotometric titration of 2×10^{-5} mol/L terpy with Tb(III) as the nitrate salt in MeCN at 298 K. **(a)** Absorption spectra and **(b)** absorbance at 335 nm with increasing Tb(III) concentration. Arrows indicate increasing and decreasing peaks.

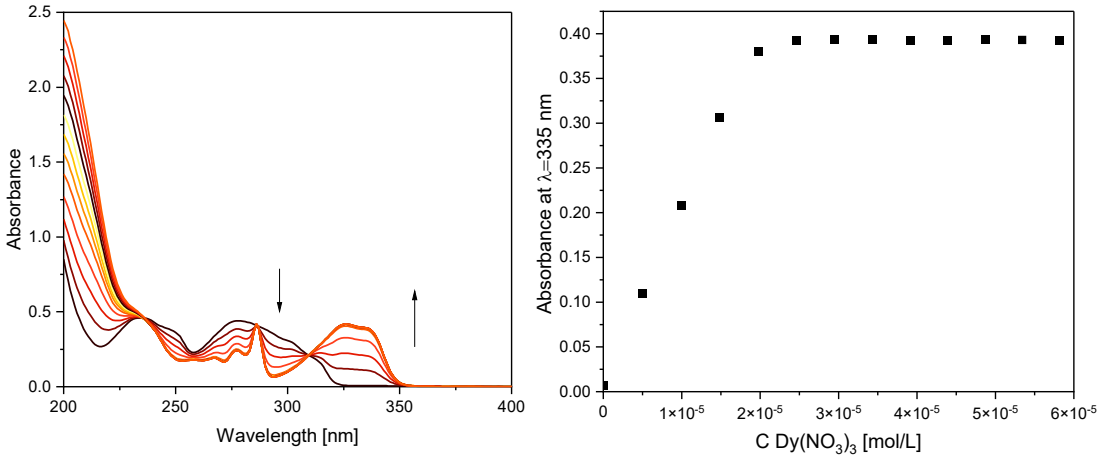

Fig. S21. Spectrophotometric titration of 2×10^{-5} mol/L terpy with Dy(III) as the nitrate salt in MeCN at 298 K. **(a)** Absorption spectra and **(b)** absorbance at 335 nm with increasing Dy(III) concentration. Arrows indicate increasing and decreasing peaks.

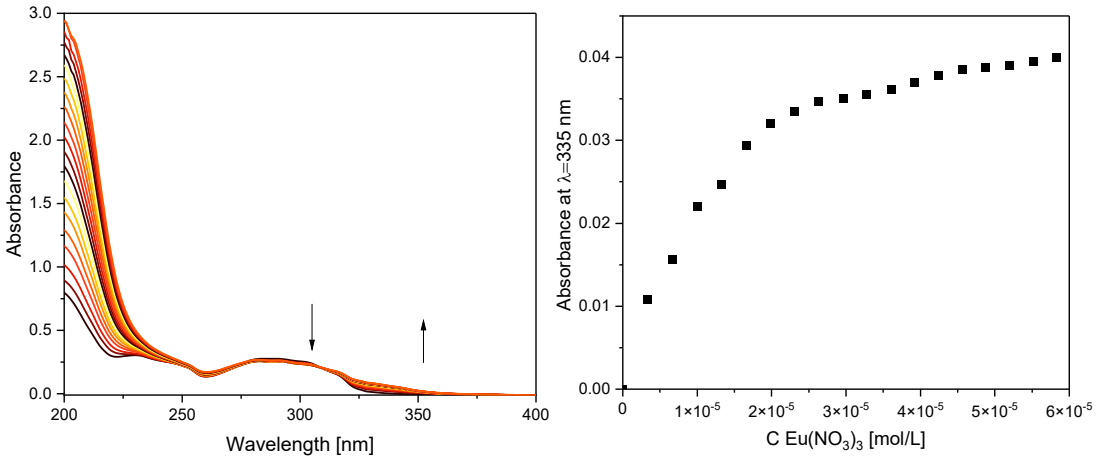

Fig. S22. Spectrophotometric titration of 2×10^{-5} mol/L terpyBr with Eu(III) as the nitrate salt in MeCN at 298 K. **(a)** Absorption spectra and **(b)** absorbance at 335 nm with increasing Eu(III) concentration. Arrows indicate increasing and decreasing peaks.

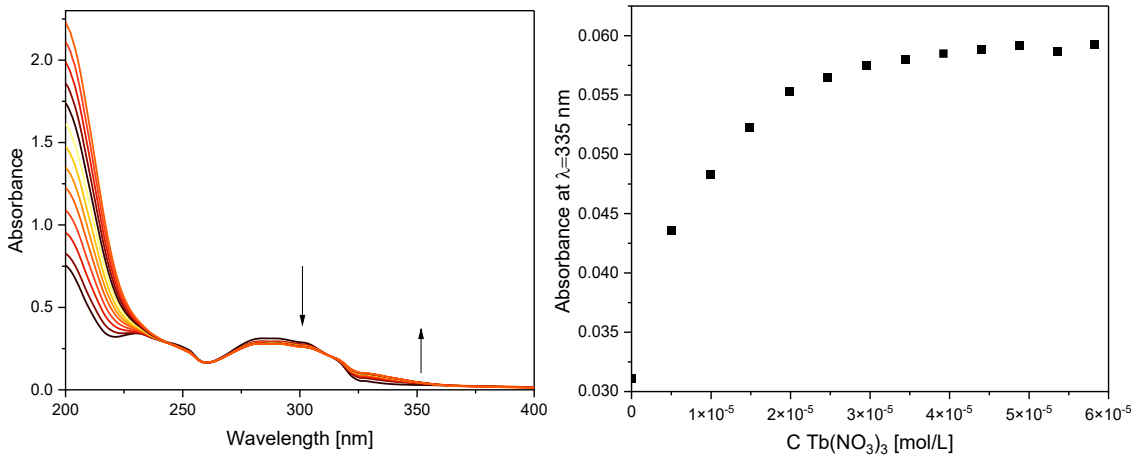

(a) **(b)**

Fig. S23. Spectrophotometric titration of 2×10^{-5} mol/L terpyBr with Tb(III) as the nitrate salt in MeCN at 298 K. **(a)** Absorption spectra and **(b)** absorbance at 335 nm with increasing Tb(III) concentration. Arrows indicate increasing and decreasing peaks.

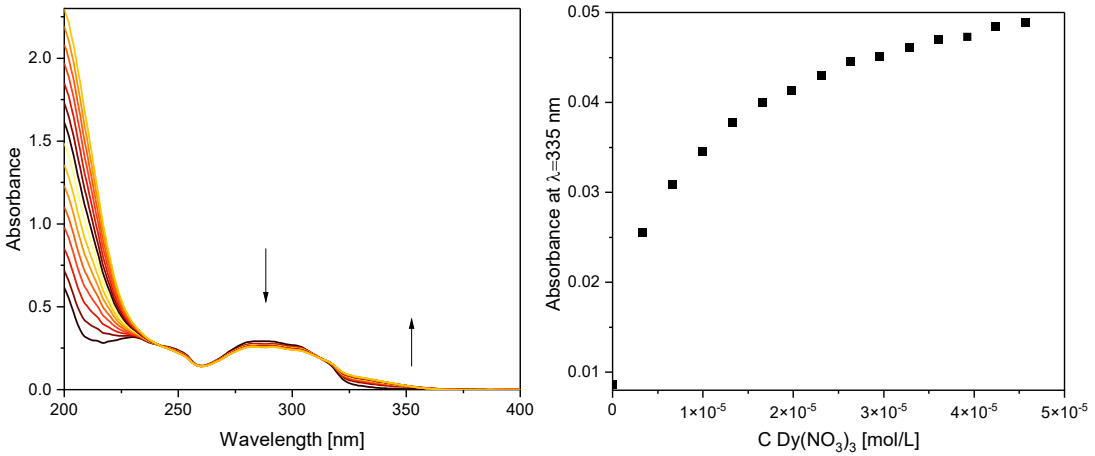

(a) **(b)**

Fig. S24. Spectrophotometric titration of 2×10^{-5} mol/L terpyBr with Dy(III) as the nitrate salt in MeCN at 298 K. **(a)** Absorption spectra and **(b)** absorbance at 335 nm with increasing Dy(III) concentration. Arrows indicate increasing and decreasing peaks.

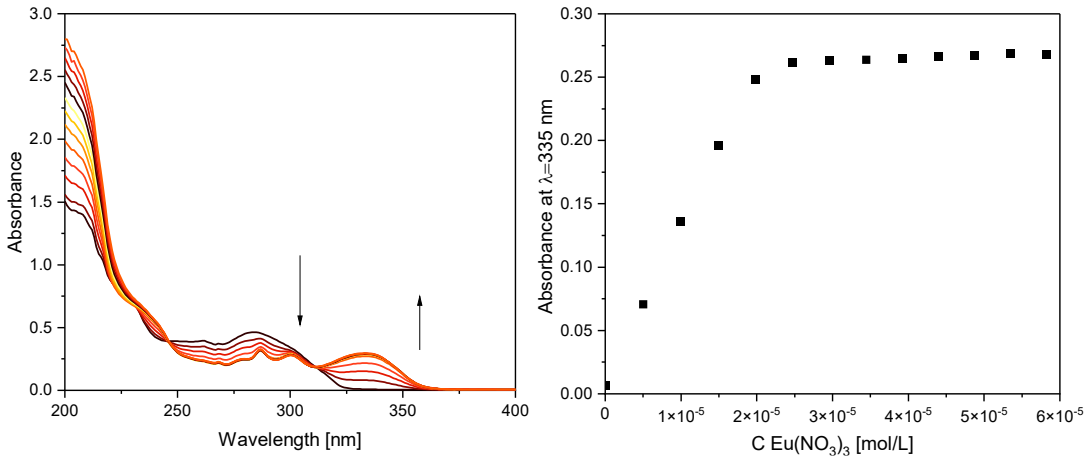

(a) **(b)**

Fig. S25. Spectrophotometric titration of 2×10^{-5} mol/L terpyCHO with Eu(III) as the nitrate salt in MeCN at 298 K. **(a)** Absorption spectra and **(b)** absorbance at 335 nm with increasing Eu(III) concentration. Arrows indicate increasing and decreasing peaks.

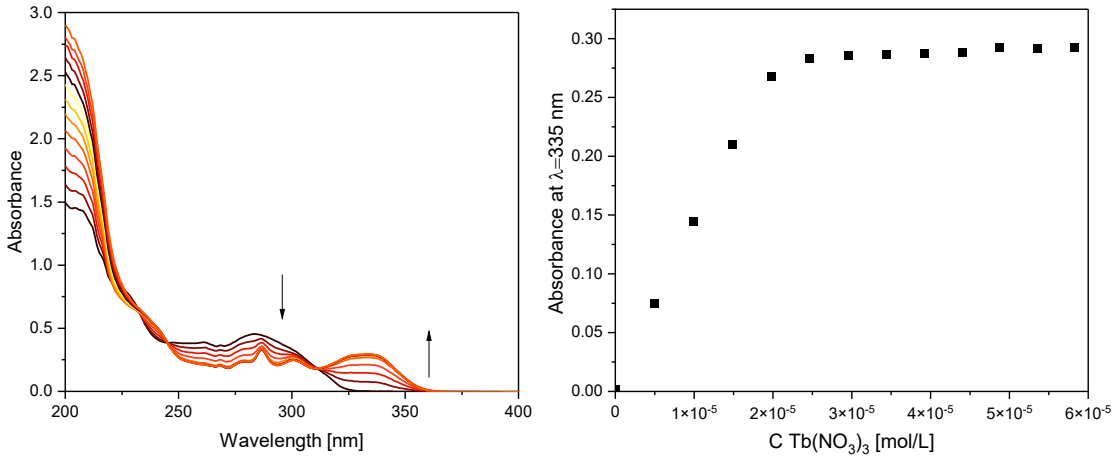

(a) **(b)**

Fig. S26. Spectrophotometric titration of 2×10^{-5} mol/L terpyCHO with Tb(III) as the nitrate salt in MeCN at 298 K. **(a)** Absorption spectra and **(b)** absorbance at 335 nm with increasing Tb(III) concentration. Arrows indicate increasing and decreasing peaks.

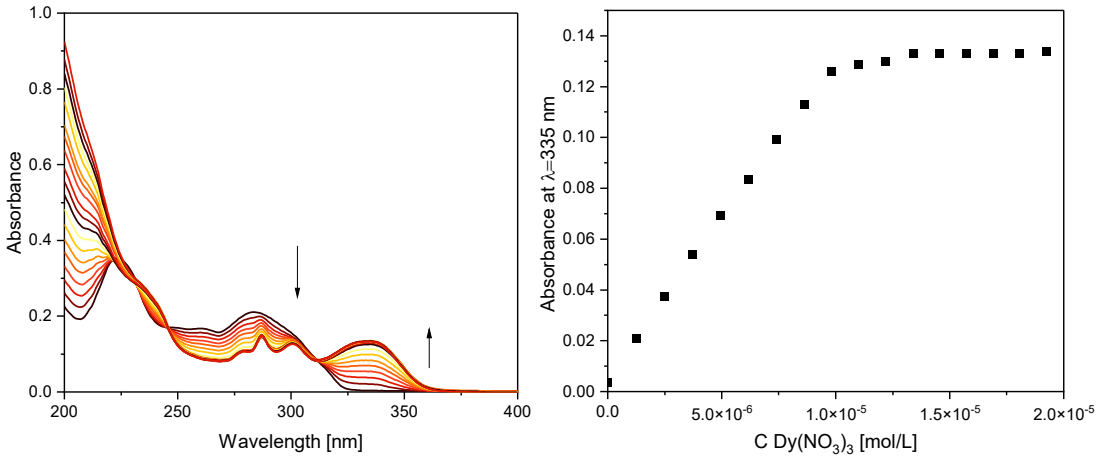

Fig. S27. Spectrophotometric titration of 2×10^{-5} mol/L terpyCHO with Dy(III) as the nitrate salt in MeCN at 298 K. **(a)** Absorption spectra and **(b)** absorbance at 335 nm with increasing Dy(III) concentration. Arrows indicate increasing and decreasing peaks.

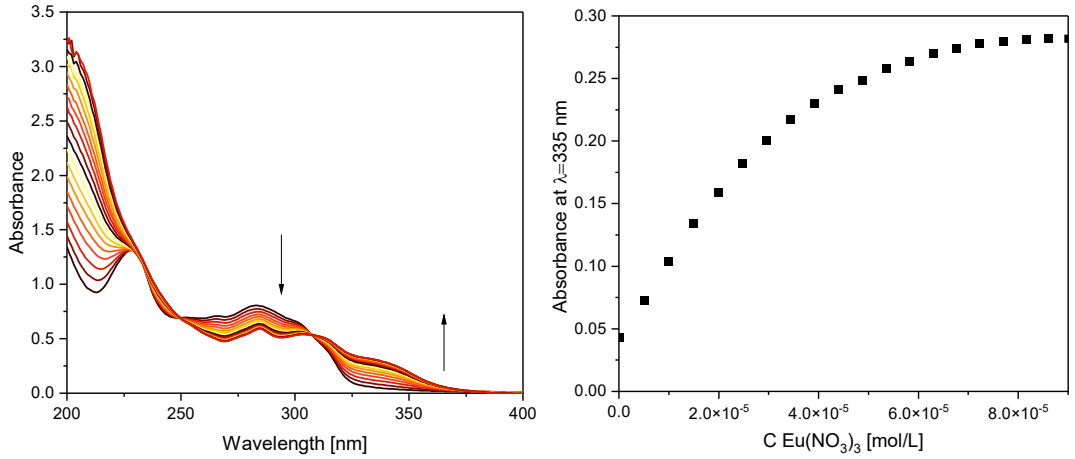

Fig. S28. Spectrophotometric titration of 4×10^{-5} mol/L terpyNO_2 with Eu(III) as the nitrate salt in MeCN at 298 K. **(a)** Absorption spectra and **(b)** absorbance at 335 nm with increasing Eu(III) concentration. Arrows indicate increasing and decreasing peaks.

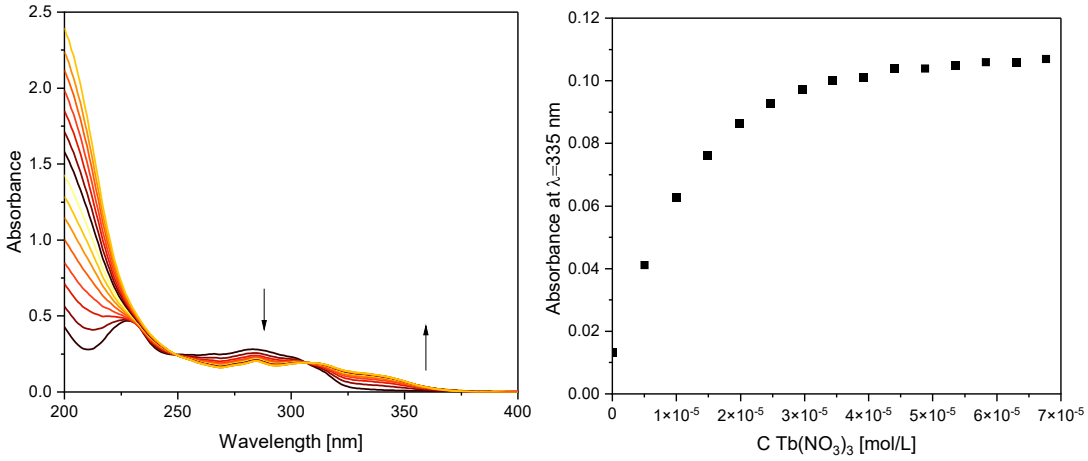

(a) **(b)**

Fig. S29. Spectrophotometric titration of 2×10^{-5} mol/L terpyNO$_2$ with Tb(III) as the nitrate salt in MeCN at 298 K. **(a)** Absorption spectra and **(b)** absorbance at 335 nm with increasing Tb(III) concentration. Arrows indicate increasing and decreasing peaks.

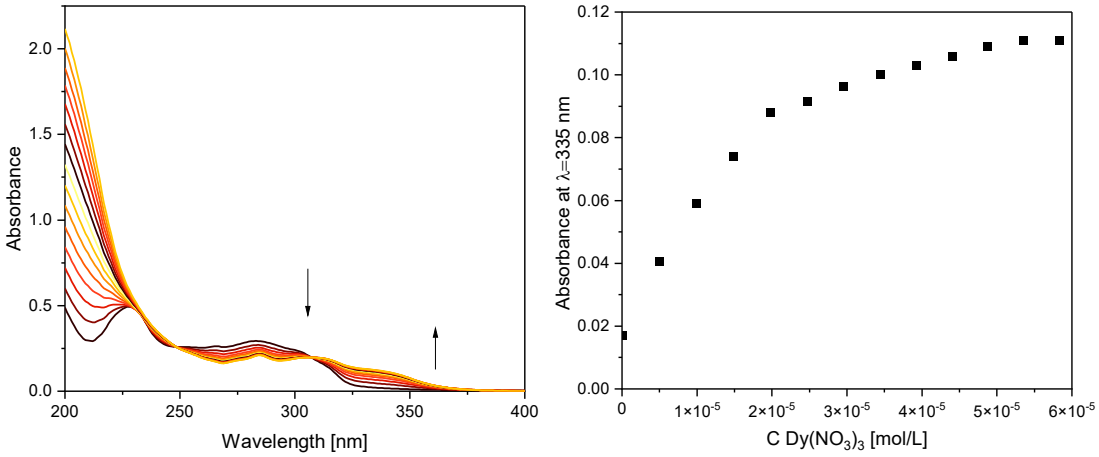

(a) **(b)**

Fig. 30. Spectrophotometric titration of 2×10^{-5} mol/L terpyNO$_2$ with Dy(III) as the nitrate salt in MeCN at 298 K. **(a)** Absorption spectra and **(b)** absorbance at 335 nm with increasing Dy(III) concentration. Arrows indicate increasing and decreasing peaks.

Photophysical Characterization

Excitation, emission and absorbance spectra of [Ln(terpyR)(NO$_3$)$_3$] complexes (298 K)

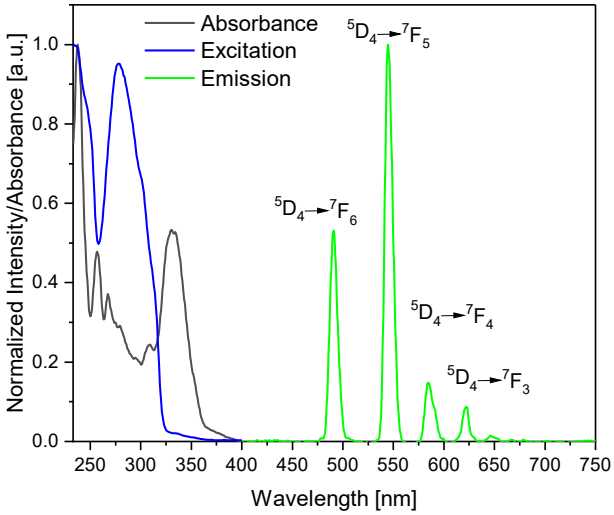

Fig. S31. Normalized excitation (blue), emission (green) and absorbance (black) spectra of 1×10^{-4} mol/L of [Tb(terpy)(NO$_3$)$_3$] in acetonitrile at 298 K, λ_{exc} = 335 nm, λ_{em} = 545 nm; slit widths excitation = 5 nm and emission = 5 nm; scan rate = 250 nm/min; gain = 775 V.

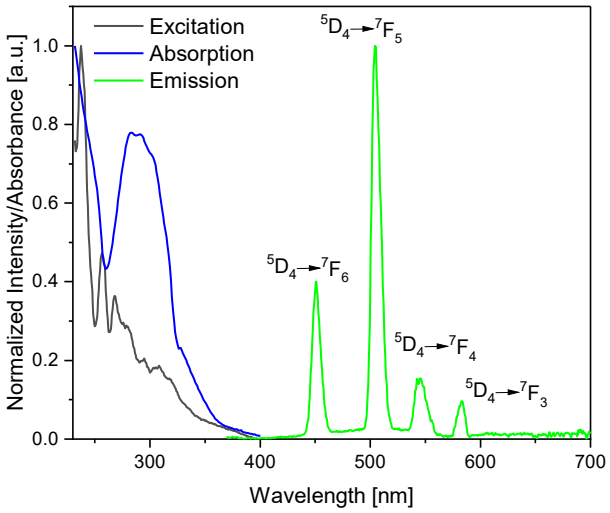

Fig. S32. Normalized excitation (blue), emission (green) and absorbance (black) spectra of 1×10^{-4} mol/L of [Tb(terpyBr)(NO$_3$)$_3$] in acetonitrile at 298 K, λ_{exc} = 335 nm, λ_{em} = 545 nm; slit widths excitation = 5 nm and emission = 5 nm; scan rate = 250 nm/min; gain = 775 V

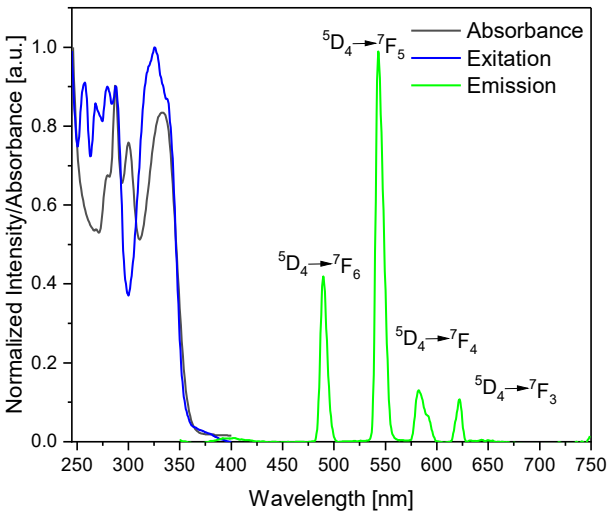

Fig. S33. Normalized excitation (blue), emission (green) and absorbance (black) spectra of 1×10^{-4} mol/L of [Tb(terpyCHO)$(NO_3)_3$] in acetonitrile at 298 K, λ_{exc} = 335 nm, λ_{em} = 545 nm; slit widths excitation = 5 nm and emission = 5 nm; scan rate = 250 nm/min; gain = 775 V

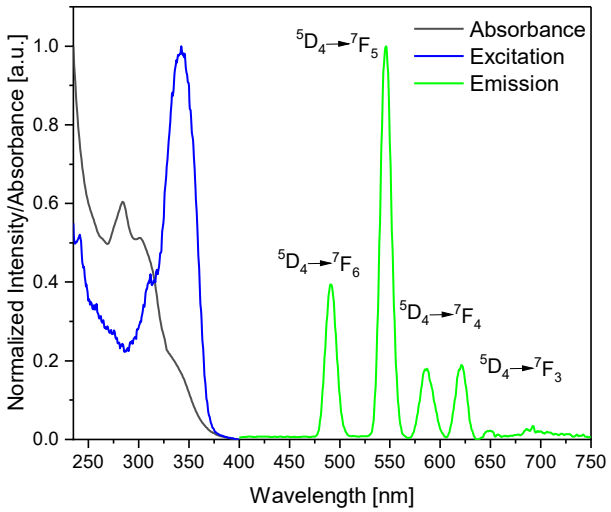

Fig. S34. Normalized excitation (blue), emission (green) and absorbance (black) spectra of 1×10^{-4} mol/L of [Tb(terpyNO_2)$(NO_3)_3$] in acetonitrile at 298 K, λ_{exc} = 335 nm, λ_{em} = 545 nm; slit widths excitation = 5 nm and emission = 5 nm; scan rate = 250 nm/min; gain = 775 V

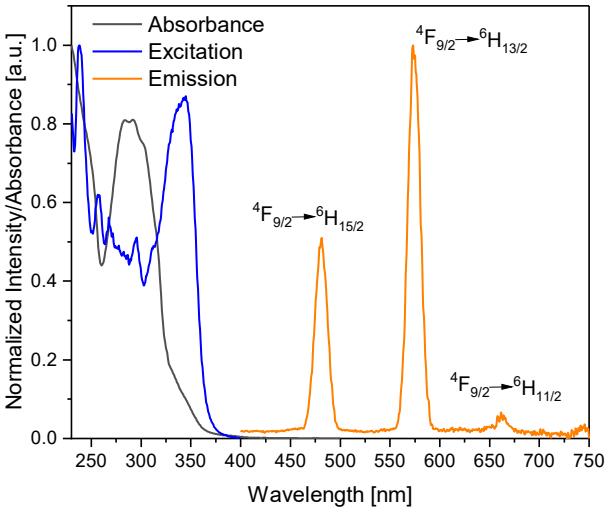

Fig. S35. Normalized excitation (blue), emission (orange), absorbance (black) spectra of 1×10^{-4} mol/L of [Dy(terpyBr)$(NO_3)_3$] in acetonitrile at 298 K, λ_{exc} = 335 nm, λ_{em} = 575 nm; slit widths excitation = 5 nm and emission = 5 nm; scan rate = 250 nm/min; gain = 775 V

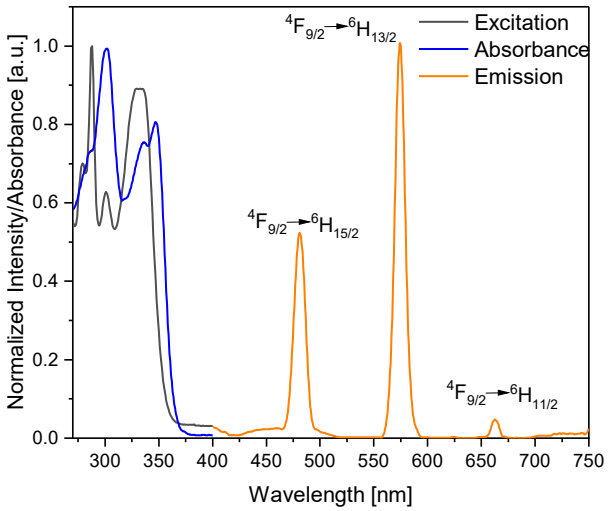

Fig. S36. Normalized excitation (blue), emission (orange), absorbance (black) spectra of 1×10^{-4} mol/L of [Dy(terpyCHO)$(NO_3)_3$] in acetonitrile at 298 K, λ_{exc} = 335 nm, λ_{em} = 575 nm; slit widths excitation = 5 nm and emission = 5 nm; scan rate = 250 nm/min; gain = 775 V

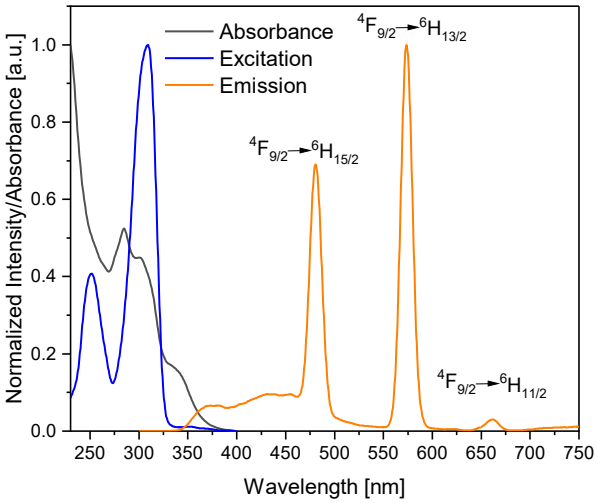

Fig. S37. Normalized excitation (blue), emission (orange), absorbance (black) spectra of 1×10^{-4} mol/L of [Dy(terpyNO$_2$)(NO$_3$)$_3$] in acetonitrile at 298 K, λ_{exc} = 335 nm, λ_{em} = 575 nm; slit widths excitation = 5 nm and emission = 5 nm; scan rate = 250 nm/min; gain = 775 V

Excitation and emission spectra of [Ln(terpyR)(NO$_3$)$_3$] complexes (77 K)

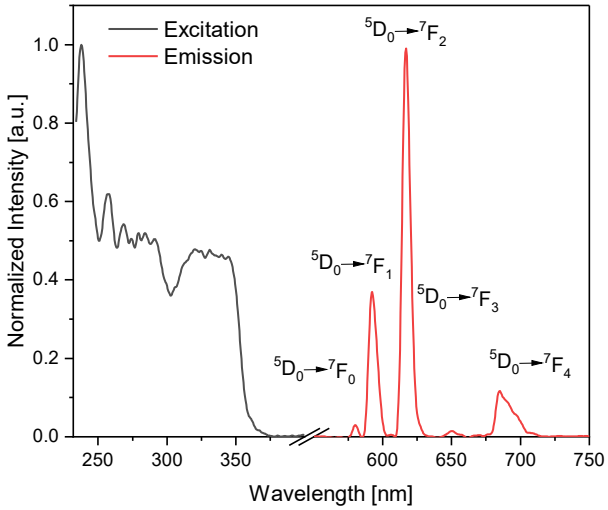

Fig. S38. Normalized excitation, emission spectra of 1×10^{-4} mol/L of [Eu(terpy)(NO$_3$)$_3$] in acetonitrile at 77 K, λ_{exc} = 335 nm, λ_{em} = 617 nm; slit widths excitation = 10 nm and emission = 2.5 nm; scan rate = 250 nm/min; gain = 775 V.

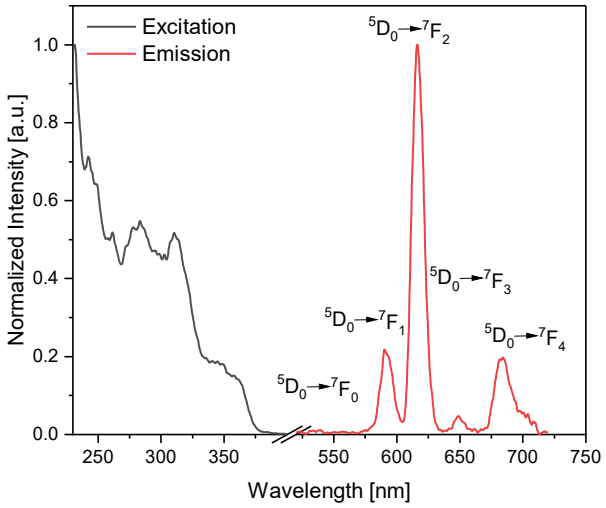

Fig. S39. Normalized excitation, emission spectra of 1×10^{-4} mol/L of [Eu(terpyBr)$(NO_3)_3$] in acetonitrile at 77 K, λ_{exc} = 335 nm, λ_{em} = 617 nm; slit widths excitation = 10 nm and emission = 2.5 nm; scan rate = 250 nm/min; gain = 775 V.

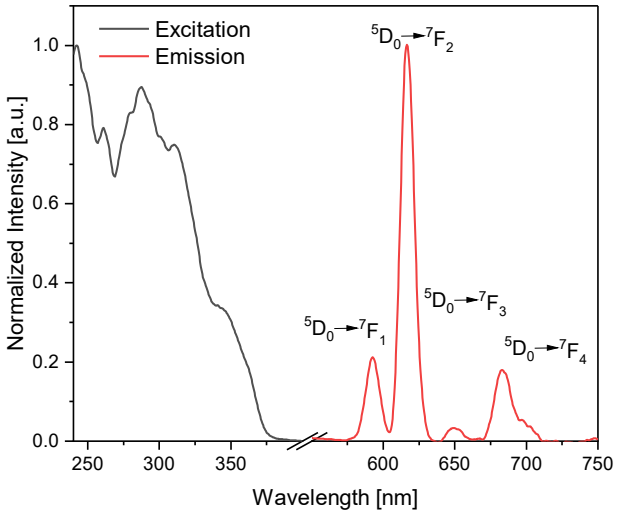

Fig. S40. Normalized excitation, emission spectra of 1×10^{-4} mol/L of [Eu(terpyCHO)$(NO_3)_3$] in acetonitrile at 77 K, λ_{exc} = 335 nm, λ_{em} = 617 nm; slit widths excitation = 10 nm and emission = 2.5 nm; scan rate = 250 nm/min; gain = 775 V.

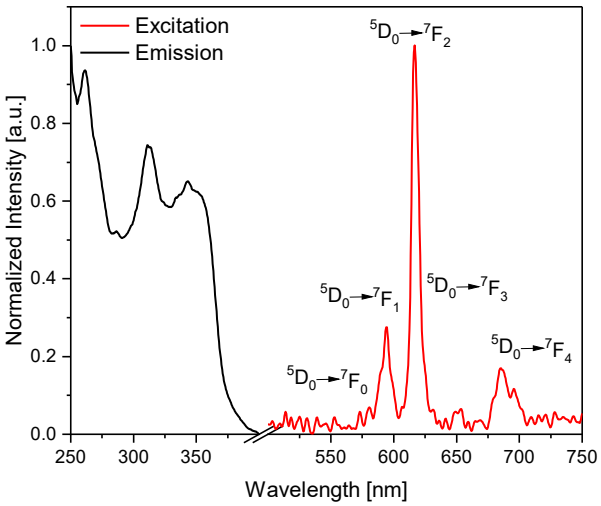

Fig. S41. Normalized excitation, emission spectra of 1×10^{-4} mol/L of $[Eu(terpyNO_2)(NO_3)_3]$ in acetonitrile at 77 K, λ_{exc} = 335 nm, λ_{em} = 617 nm; slit widths excitation = 10 nm and emission = 2.5 nm; scan rate = 250 nm/min; gain = 775 V.

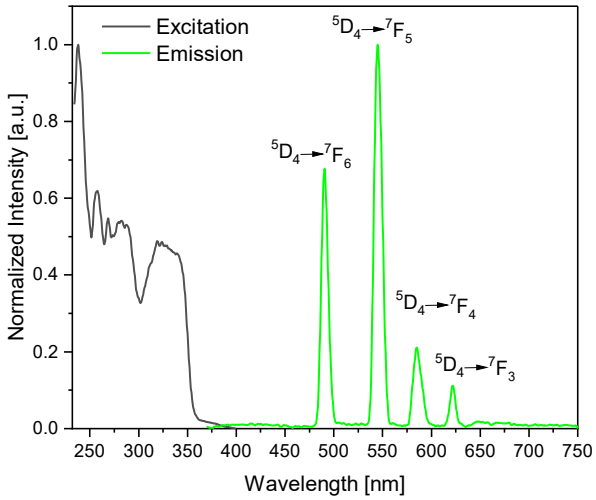

Fig. S42. Normalized excitation, emission spectra of 1×10^{-4} mol/L of $[Tb(terpy)(NO_3)_3]$ in acetonitrile at 77 K, λ_{exc} = 335 nm, λ_{em} = 545 nm; slit widths excitation = 10 nm and emission = 2.5 nm; scan rate = 250 nm/min; gain = 775 V.

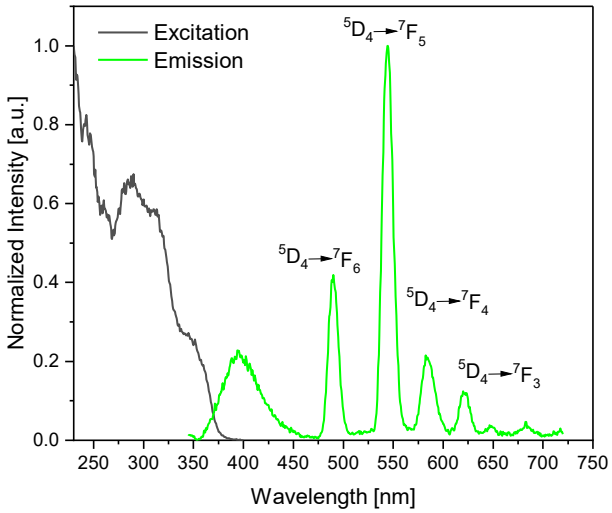

Fig. S43. Normalized excitation, emission spectra of 1×10^{-4} mol/L of [Tb(terpyBr)$(NO_3)_3$] in acetonitrile at 77 K, λ_{exc} = 335 nm, λ_{em} = 545 nm; slit widths excitation = 10 nm and emission = 2.5 nm; scan rate = 250 nm/min; gain = 775 V.

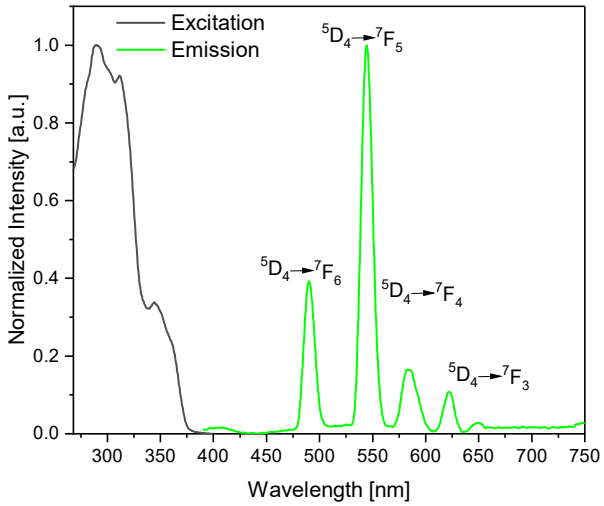

Fig. S44. Normalized excitation, emission spectra of 1×10^{-4} mol/L of [Tb(terpyCHO)$(NO_3)_3$] in acetonitrile at 77 K, λ_{exc} = 335 nm, λ_{em} = 545 nm; slit widths excitation = 10 nm and emission = 2.5 nm; scan rate = 250 nm/min; gain = 775 V.

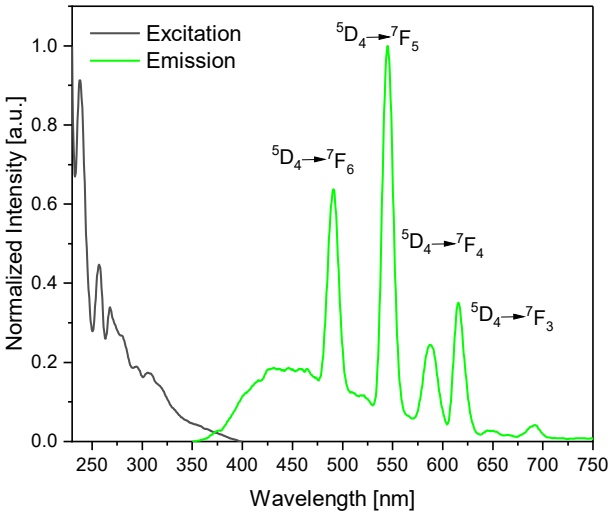

Fig. S45. Normalized excitation, emission spectra of 1×10^{-4} mol/L of [Tb(terpyNO$_2$)(NO$_3$)$_3$] in acetonitrile at 77 K, λ_{exc} = 335 nm, λ_{em} = 545 nm; slit widths excitation = 10 nm and emission = 2.5 nm; scan rate = 250 nm/min; gain = 775 V.

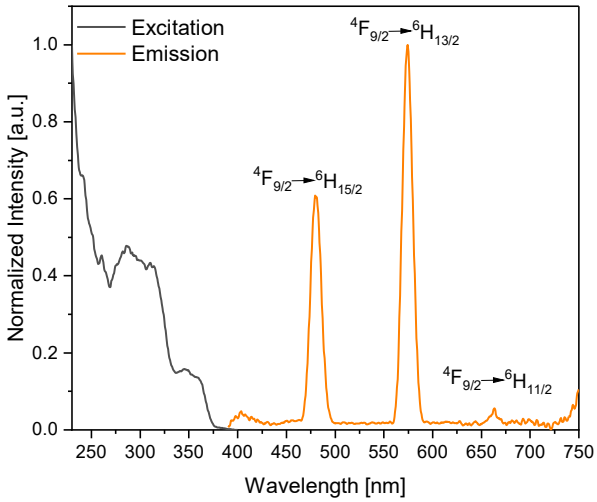

Fig. S46. Normalized excitation, emission spectra of 1×10^{-4} mol/L of [Dy(terpyBr)(NO$_3$)$_3$] in acetonitrile at 77 K, λ_{exc} =335 nm, λ_{em} = 575 nm; slit widths excitation = 10 nm and emission = 2.5 nm; scan rate = 250 nm/min; gain = 775 V.

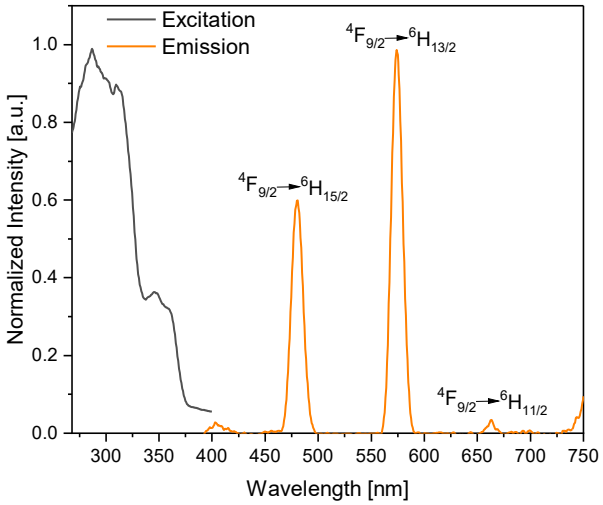

Fig. S47. Normalized excitation, emission spectra of 1×10^{-4} mol/L of [Dy(terpyCHO)$(NO_3)_3$] in acetonitrile at 77 K, λ_{exc} =335 nm, λ_{em} = 575 nm; slit widths excitation = 10 nm and emission = 2.5 nm; scan rate = 250 nm/min; gain = 775 V.

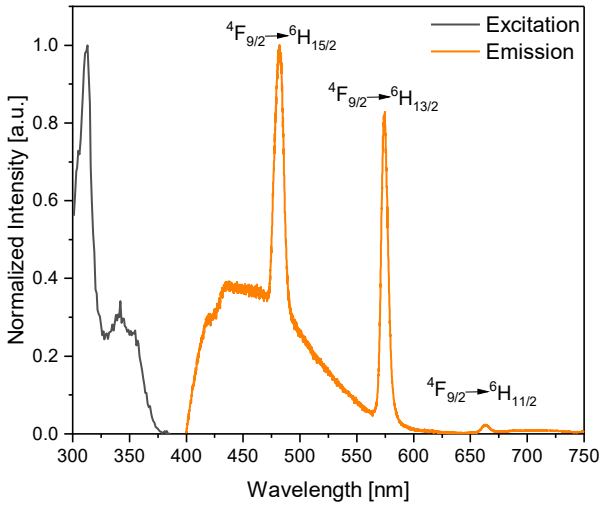

Fig. S48. Normalized excitation, emission spectra of 1×10^{-4} mol/L of [Dy(terpyNO_2)$(NO_3)_3$] in acetonitrile at 77 K, λ_{exc} =335 nm, λ_{em} = 575 nm; slit widths excitation = 9 nm and emission = 9 nm; scan rate = 250 nm/min; gain = 775 V.

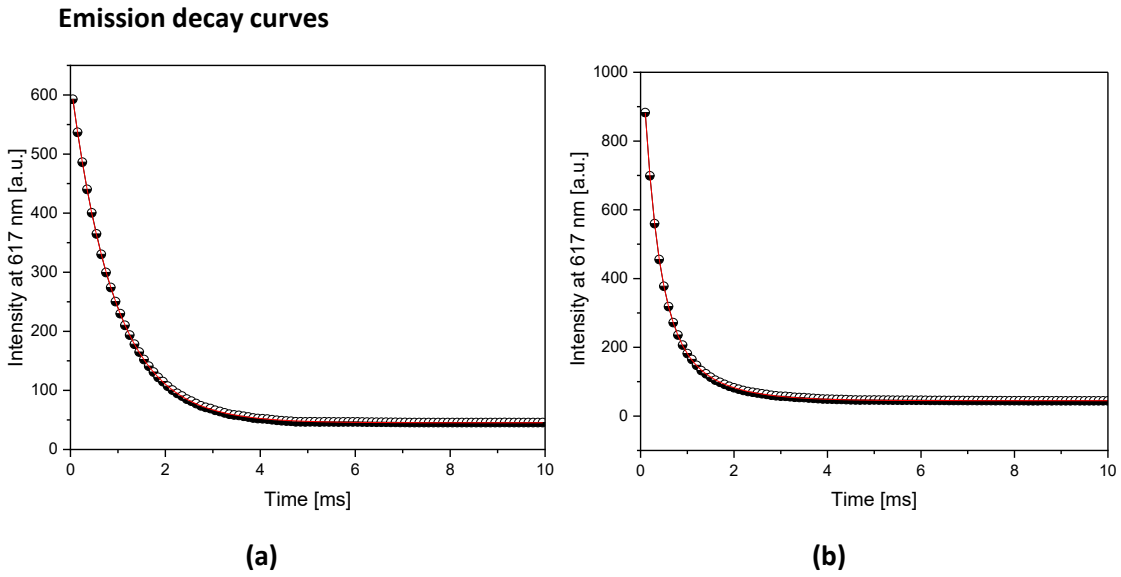

Fig. S49. Luminescence intensity decay plot of [Eu(terpy)$(NO_3)_3$] at 617 nm ($^5D_0 \rightarrow {}^7F_2$). (**a**) Fit to a single exponential function in acetonitrile at 298 K and (**b**) fit to a double exponential function in acetonitrile at 77 K. [Complex] = 1×10^{-4} mol/L; λ_{exc} = 335 nm; slit widths excitation = 10 nm and emission = 2.5 nm; scan rate = 250 nm/min; gain = 775 V.

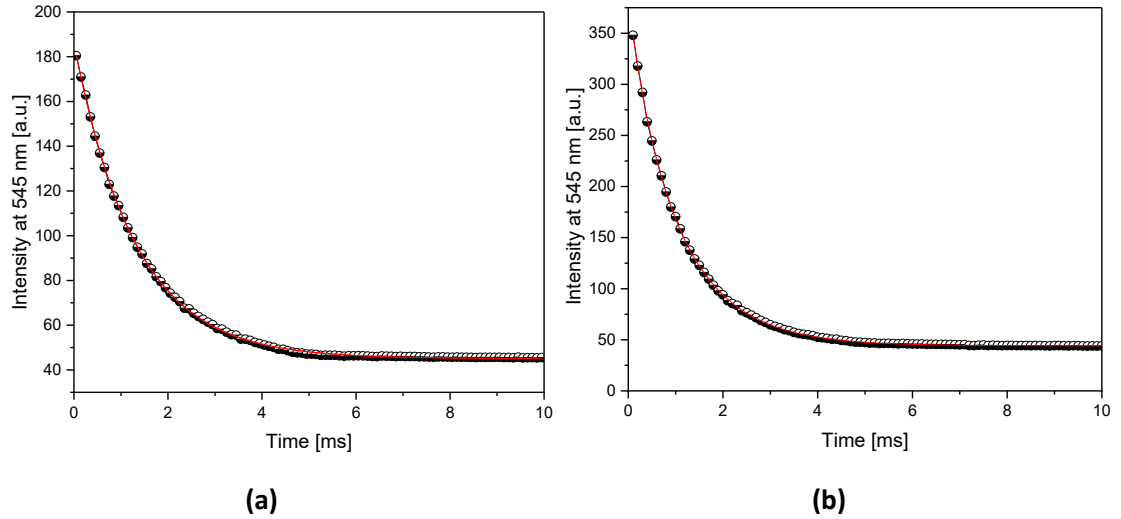

Fig. S50. Luminescence intensity decay plot of [Tb(terpy)$(NO_3)_3$] at 545 nm ($^5D_4 \rightarrow {}^7F_5$). (**a**) Fit to a single exponential function in acetonitrile at 298 K and (**b**) fit to a double exponential function in acetonitrile at 77 K. [Complex] = 1×10^{-4} mol/L; λ_{exc} = 335 nm; slit widths excitation = 10 nm and emission = 2.5 nm; scan rate = 250 nm/min; gain = 775 V.

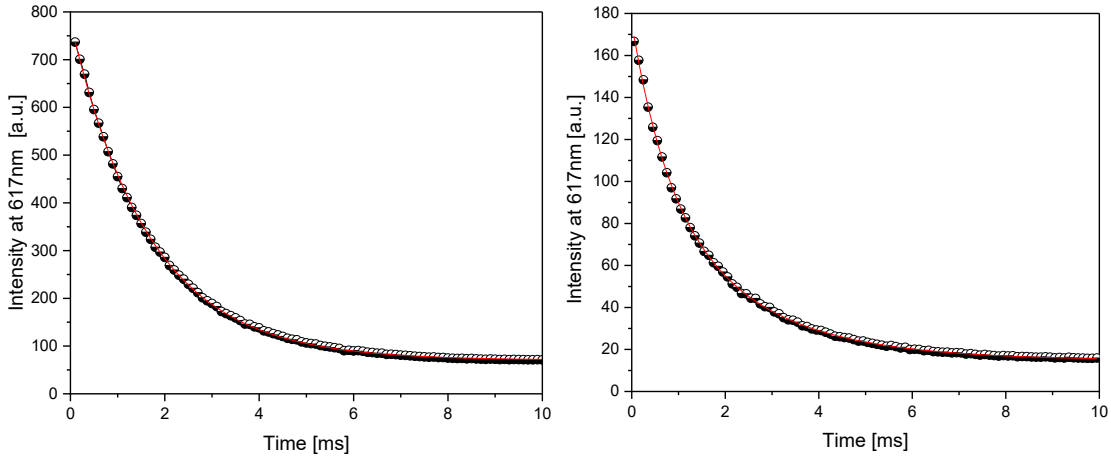

Fig. S51. Luminescence intensity decay plot of [Eu(terpyBr)$(NO_3)_3$] at 617 nm ($^5D_0 \rightarrow {}^7F_2$). (**a**) Fit to a single exponential function in acetonitrile at 298 K and (**b**) fit to a double exponential function in acetonitrile at 77 K. [Complex] = 1×10^{-4} mol/L; λ_{exc} = 335 nm; slit widths excitation = 10 nm and emission = 2.5 nm; scan rate = 250 nm/min; gain = 775 V.

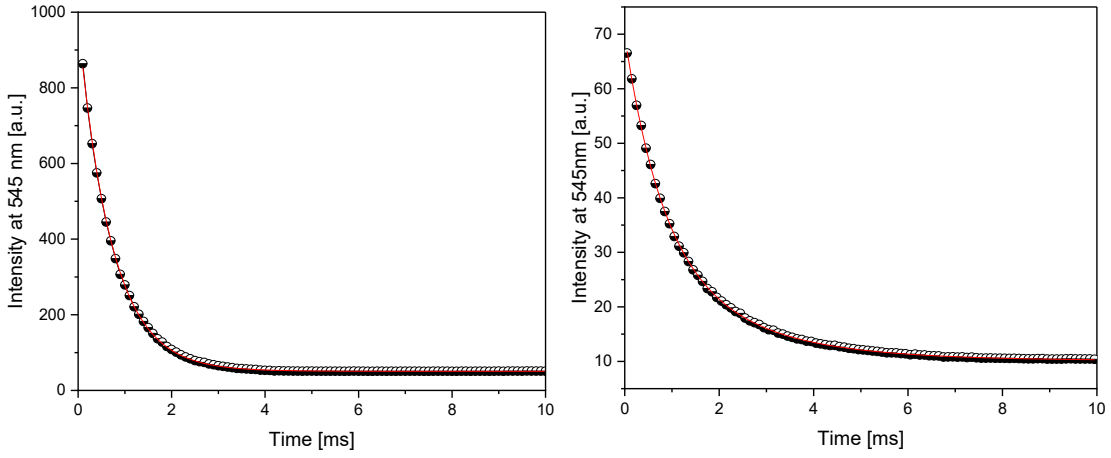

Fig. S52. Luminescence intensity decay plot of [Tb(terpyBr)$(NO_3)_3$] at 545 nm ($^5D_4 \rightarrow {}^7F_5$). (**a**) Fit to a single exponential function in acetonitrile at 298 K and (**b**) fit to a double exponential function in acetonitrile at 77 K. [Complex] = 1×10^{-4} mol/L; λ_{exc} = 335 nm; slit widths excitation= 10 nm and emission = 2.5 nm; scan rate = 250 nm/min; gain = 775 V.

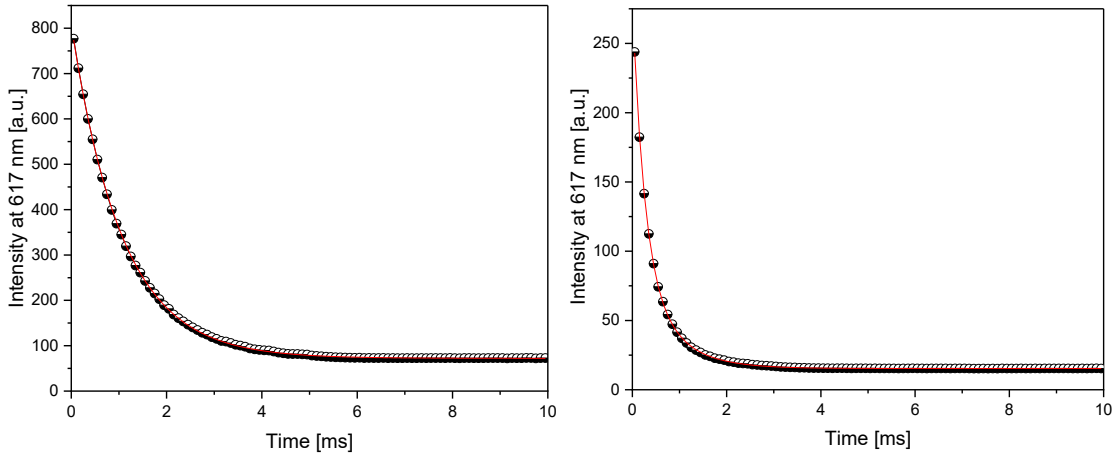

(a) **(b)**

Fig. S53. Luminescence intensity decay plot of [Eu(terpyCHO)$(NO_3)_3$] at 617 nm ($^5D_0 \rightarrow {}^7F_2$). (**a**) Fit to a single exponential function in acetonitrile at 298 K and (**b**) fit to a double exponential function in acetonitrile at 77 K. [Complex] = 1×10^{-4} mol/L; λ_{exc} = 335 nm; slit widths excitation = 10 nm and emission = 2.5 nm; scan rate = 250 nm/min; gain = 775 V.

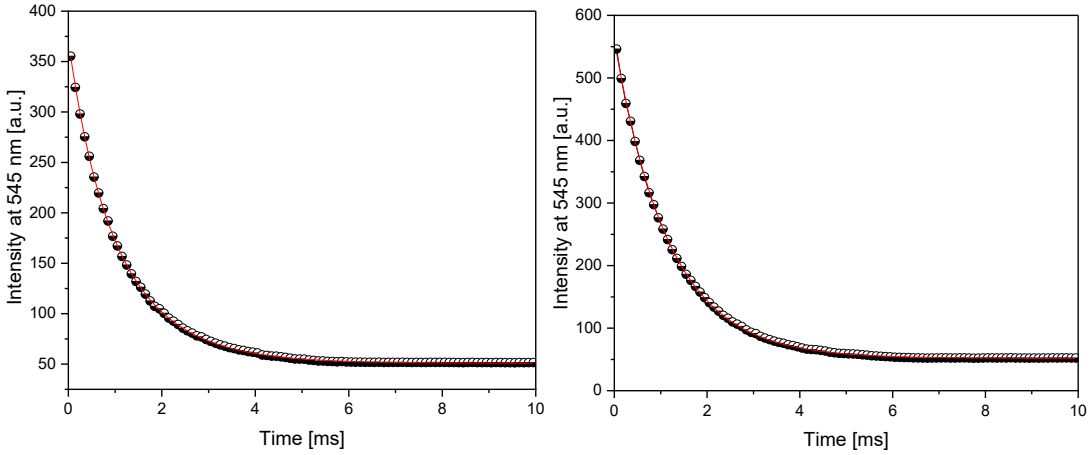

(a) **(b)**

Fig. S54. Luminescence intensity decay plot of [Tb(terpyCHO)$(NO_3)_3$] at 545 nm ($^5D_4 \rightarrow {}^7F_5$). (**a**) Fit to a single exponential function in acetonitrile at 298 K and (**b**) fit to a double exponential function in acetonitrile at 77 K. [Complex] = 1×10^{-4} mol/L; λ_{exc} = 335 nm; slit widths excitation = 10 nm and emission = 2.5 nm; scan rate = 250 nm/min; gain = 775 V.

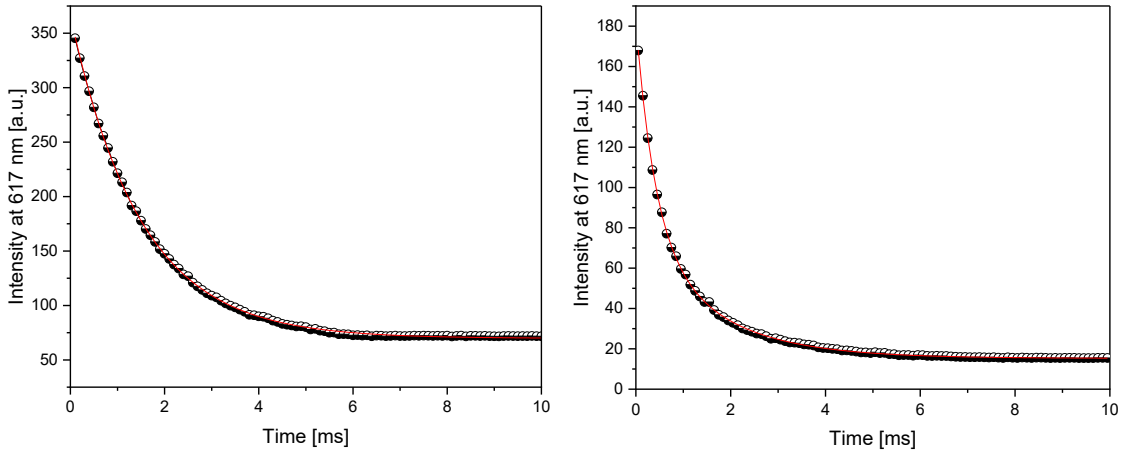

(a) **(b)**

Fig. S55. Luminescence intensity decay plot of [Eu(terpyNO$_2$)(NO$_3$)$_3$] at 617 nm ($^5D_0 \rightarrow {}^7F_2$). (**a**) Fit to a single exponential function in acetonitrile at 298 K and (**b**) fit to a double exponential function in acetonitrile at 77 K. [Complex] = 1×10^{-4} mol/L; λ_{exc} = 335 nm; slit widths excitation = 10 nm and emission = 2.5 nm; scan rate = 250 nm/min; gain = 775 V.

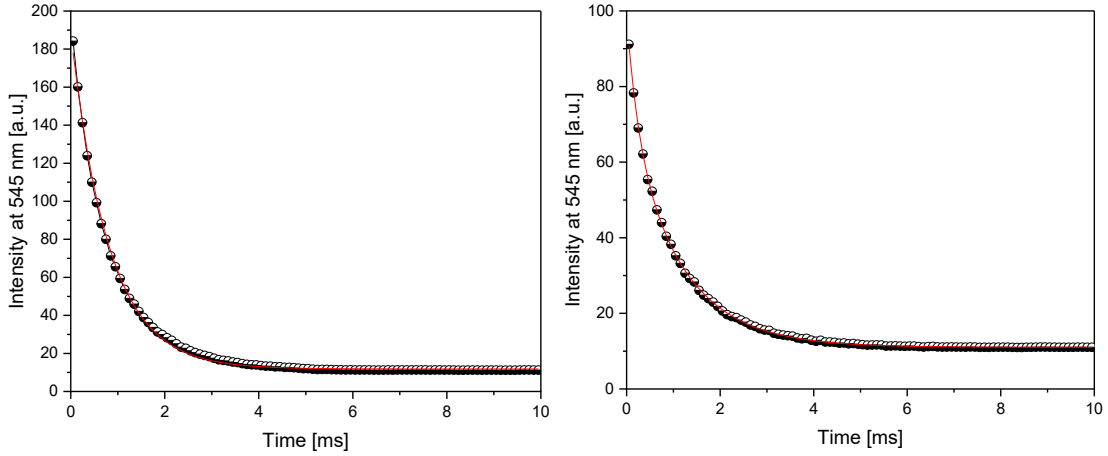

(a) **(b)**

Fig. S56. Luminescence intensity decay plot of [Tb(terpyNO$_2$)(NO$_3$)$_3$] at 545 nm ($^5D_4 \rightarrow {}^7F_5$). (**a**) Fit to a single exponential function in acetonitrile at 298 K and (**b**) fit to a double exponential function in acetonitrile at 77 K. [Complex] = 1×10^{-4} mol/L; λ_{exc} = 335 nm; slit widths excitation = 10 nm and emission = 2.5 nm; scan rate = 250 nm/min; gain = 775 V.

Fluorescence and phosphorescence spectra

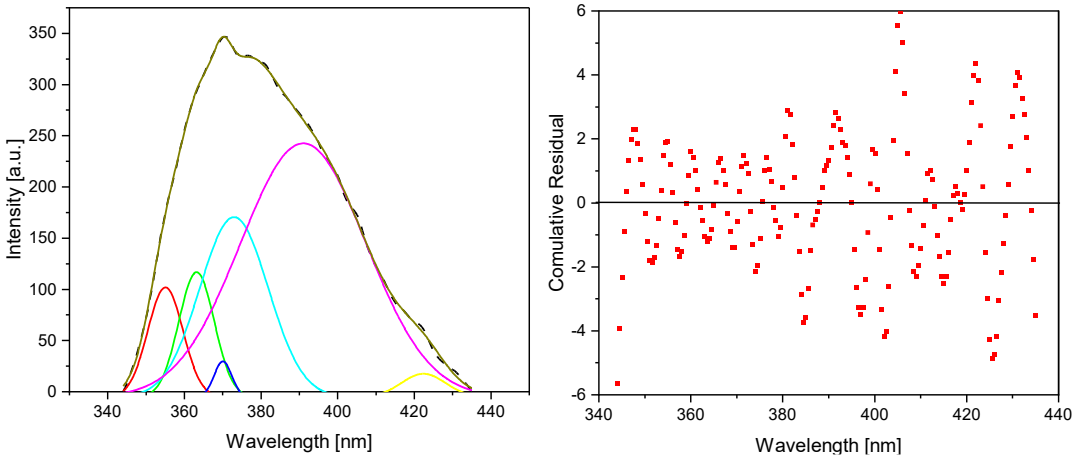

Fig. S57. (**a**) Deconvolution of the fluorescence spectrum recorded at 77 K of [Gd(terpy)$(NO_3)_3$] into its vibrational progression and (**b**) residuals of this fit. [Complex] = 1×10^{-4} mol/L; λ_{exc} = 335 nm; slit widths excitation = 10 nm and emission = 2.5 nm; scan rate = 250 nm/min; gain = 775 V.

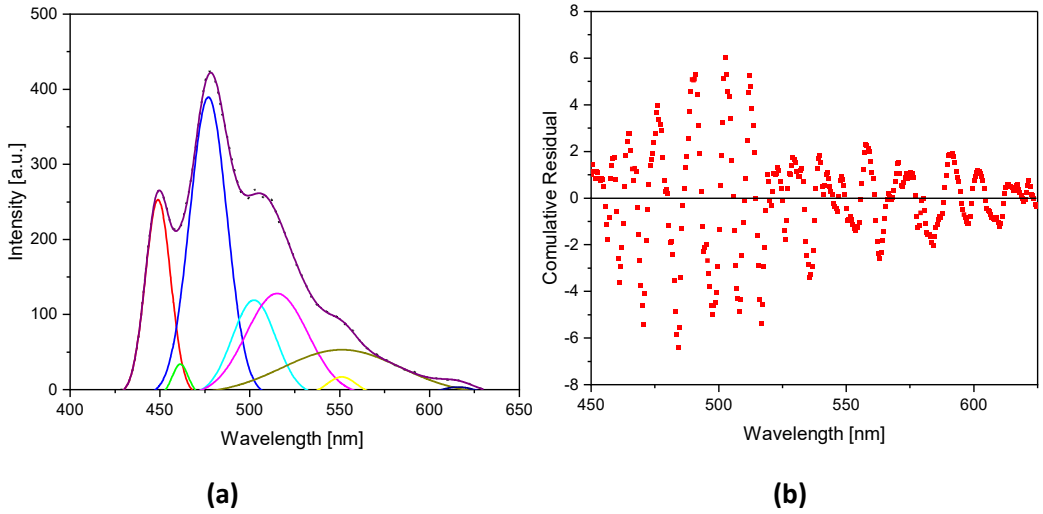

Fig. S58. (a) Deconvolution of the phosphorescence spectrum of the [Gd(terpy)$(NO_3)_3$] into its vibrational progression recorded at 77 K and (**b**) residuals of this fit. [Complex] = 1×10^{-4} mol/L; λ_{exc} = 335 nm; delay = 0.1 ms; slit widths excitation = 10 nm and emission = 2.5 nm; scan rate = 250 nm/min; gain = 775 V.

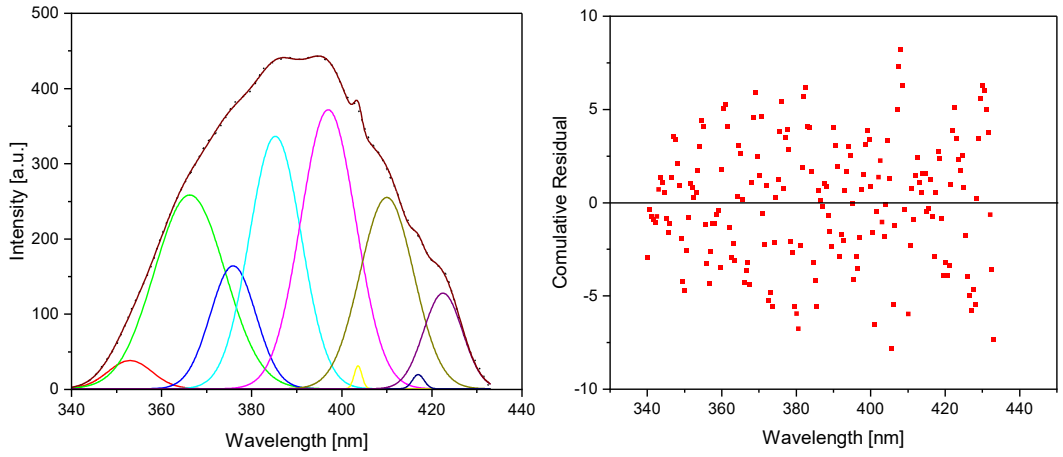

(a) **(b)**

Fig. S59. (a) Deconvolution of the fluorescence spectrum of the [Gd(terpyBr)$(NO_3)_3$] into its vibrational progression recorded at 77 K and (**b**) residuals of this fit. [Complex] = 1×10^{-4} mol/L; λ_{exc} = 335 nm; slit widths excitation = 10 nm and emission = 2.5 nm; scan rate = 250 nm/min; gain = 775 V.

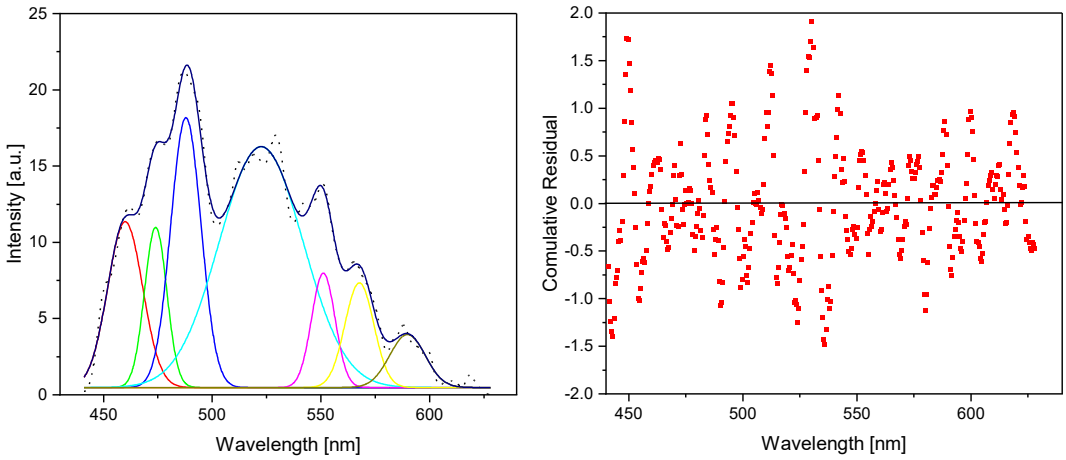

(a) **(b)**

Fig. S60. (a) Deconvolution of the phosphorescence spectrum of the [Gd(terpyBr)$(NO_3)_3$] into its vibrational progression recorded at 77 K and (**b**) residuals of this fit. [Complex] = 1×10^{-4} mol/L; λ_{exc} = 335 nm; delay = 0.03 ms; slit widths excitation = 10 nm and emission = 2.5 nm; scan rate = 250 nm/min; gain = 775 V.

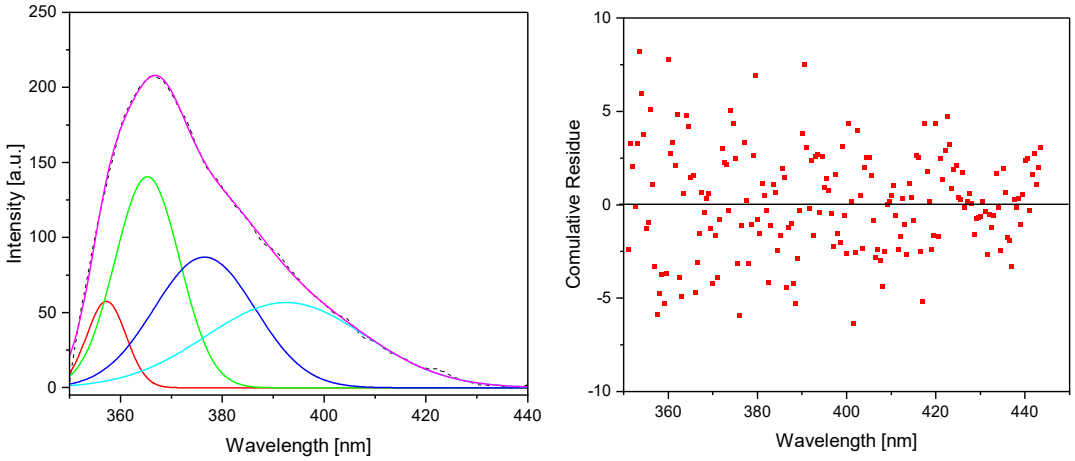

(a) **(b)**

Fig. S61. (a) Deconvolution of the fluorescence spectrum of the [Gd(terpyCHO)$(NO_3)_3$] into its vibrational progression recorded at 77 K and (**b**) residuals of this fit. [Complex] = 1×10^{-4} mol/L; λ_{exc} = 335 nm; slit widths excitation = 10 nm and emission = 2.5 nm; scan rate = 250 nm/min; gain = 775 V.

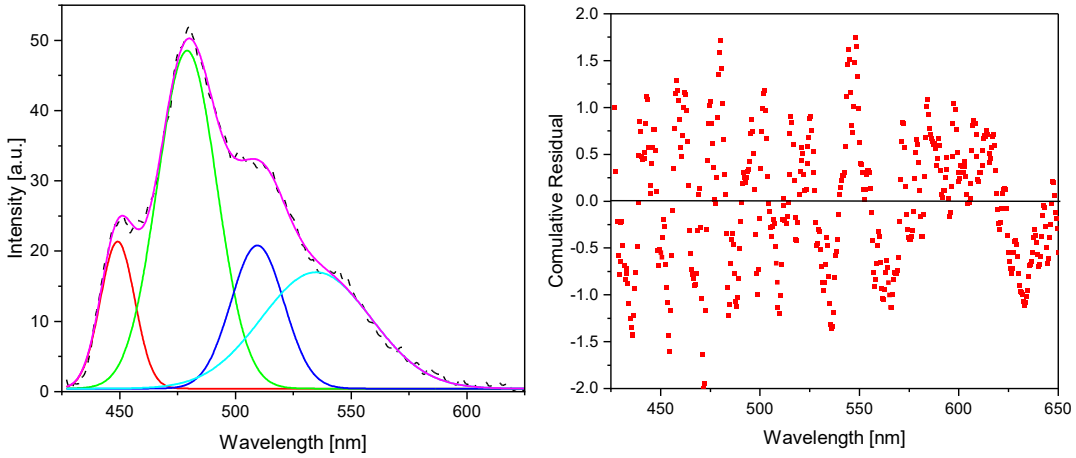

(a) **(b)**

Fig. S62. (a) Deconvolution of the phosphorescence spectrum of the [Gd(terpyCHO)$(NO_3)_3$] into its vibrational progression recorded at 77 K and (**b**) residuals of this fit. [Complex] = 1×10^{-4} mol/L; λ_{exc} = 335 nm; delay = 0.05 ms; slit widths excitation = 10 nm and emission = 2.5 nm; scan rate = 250 nm/min; gain = 775 V.

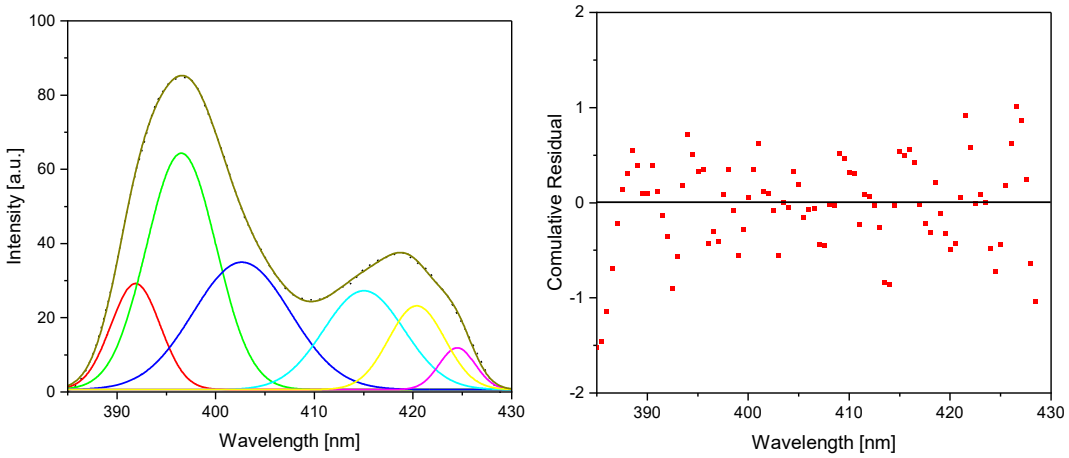

(a) **(b)**

Fig. S63. (a) Deconvolution of the fluorescence spectrum of the [Gd(terpyNO$_2$)(NO$_3$)$_3$] into its vibrational progression recorded at 77 K and (**b**) residuals of this fit. [Complex] = 1×10^{-4} mol/L; λ_{exc} = 335 nm; slit widths excitation = 10 nm and emission = 2.5 nm; scan rate = 250 nm/min; gain = 775 V.

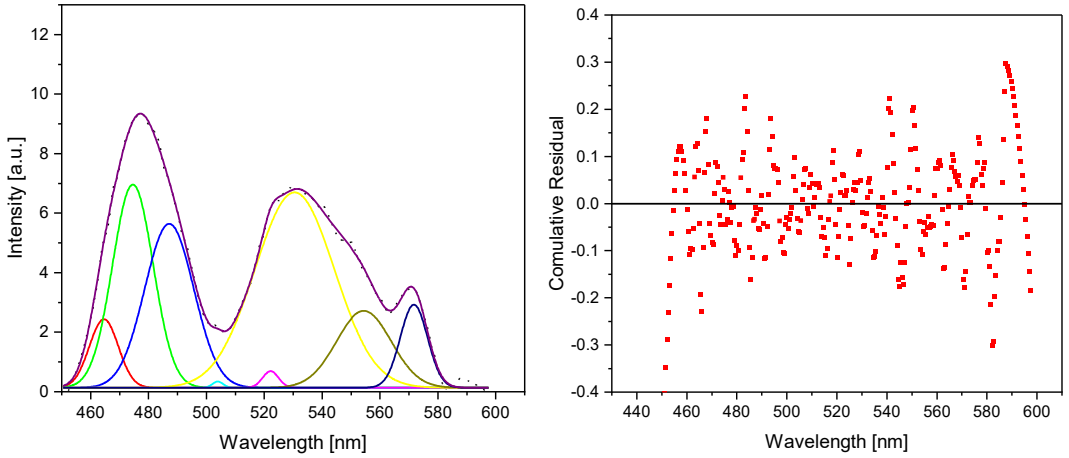

(a) **(b)**

Fig. S64. (a) Deconvolution of the phosphorescence spectrum of the [Gd(terpyNO$_2$)(NO$_3$)$_3$] into its vibrational progression recorded at 77 K and (**b**) residuals of this fit. [Complex] = 1×10^{-4} mol/L; λ_{exc} = 335 nm; delay = 0.07 ms; slit widths excitation = 10 nm and emission = 2.5 nm; scan rate = 250 nm/min; gain = 775 V.

Energy transfer rates

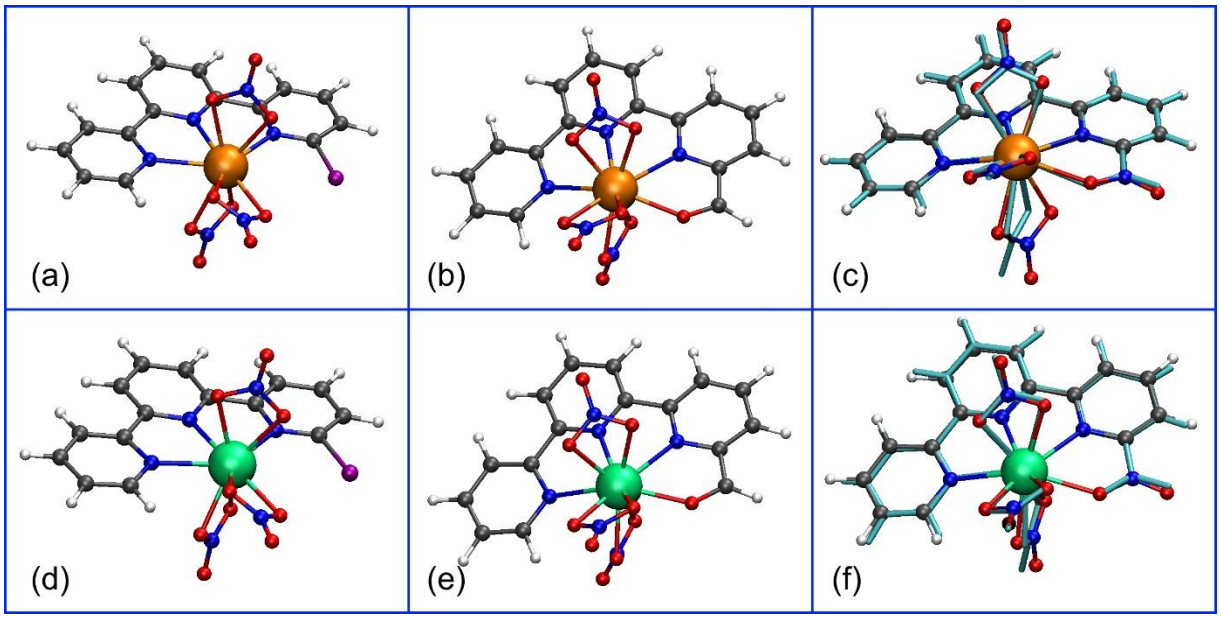

Fig. S65. Structures of complexes, optimized with the RM1-Sparkle model, used in all calculations using LUMPAC and JOYSpectra. Eu(terpyBr) (a), Eu(terpyCHO) (b), Eu(terpyNO_2) (c), Tb(terpyBr) (d), Tb(terpyCHO) (e), Tb(terpyNO_2) (f).

Atom types: hydrogen – white; carbon – black; nitrogen – blue; oxygen – red; europium – orange; terbium – green. The Eu(terpyNO_2) (c) and Tb(terpyNO_2) (f) structures were overlapped with the experimental X-ray geometries (blue framework).

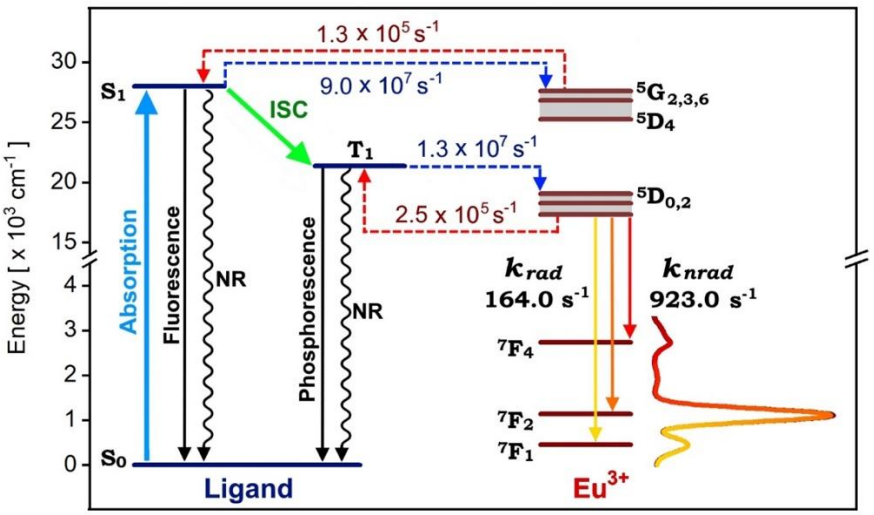

Fig. S66. Jabłoński diagram for Eu(terpy) with energy transfer (red dashed lines and numbers) and back transfer (blue dashed lines and numbers) rates.

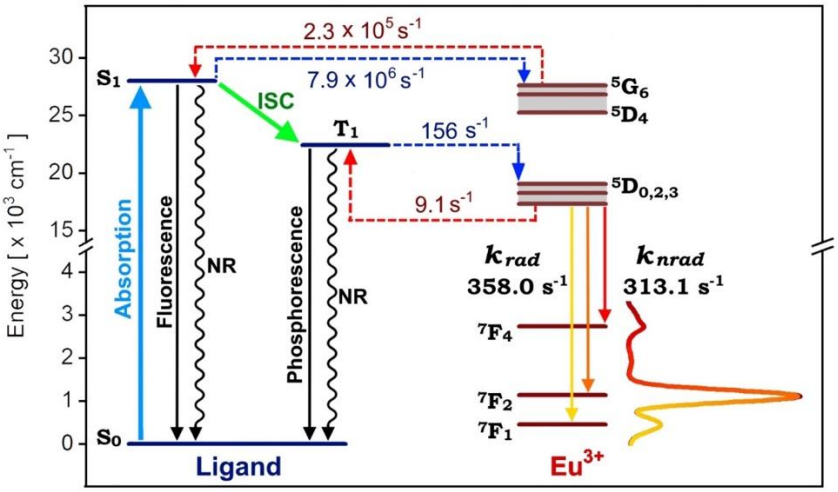

Fig. S67. Jabłoński diagram for Eu(terpyNO_2) with energy transfer (red dashed lines and numbers) and back transfer (blue dashed lines and numbers) rates.

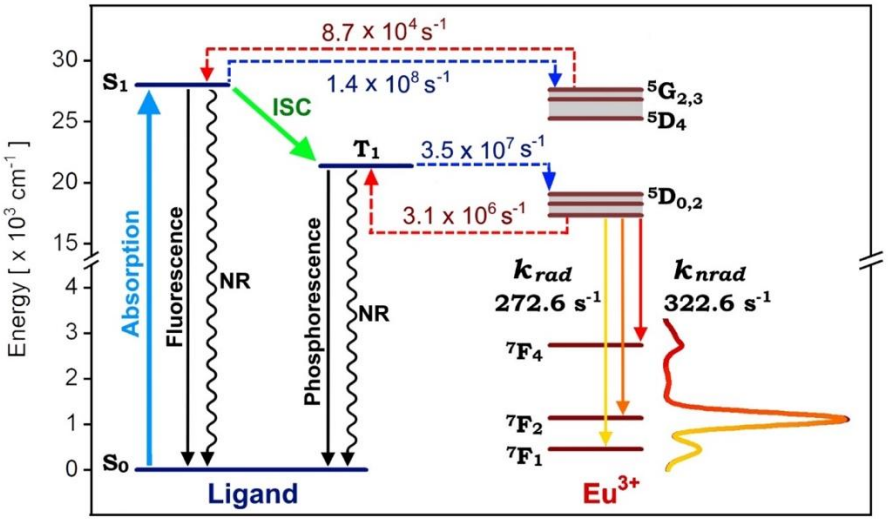

Fig. S68. Jabłoński diagram for Eu(terpyCHO) with energy transfer (red dashed lines and numbers) and back transfer (blue dashed lines and numbers) rates.

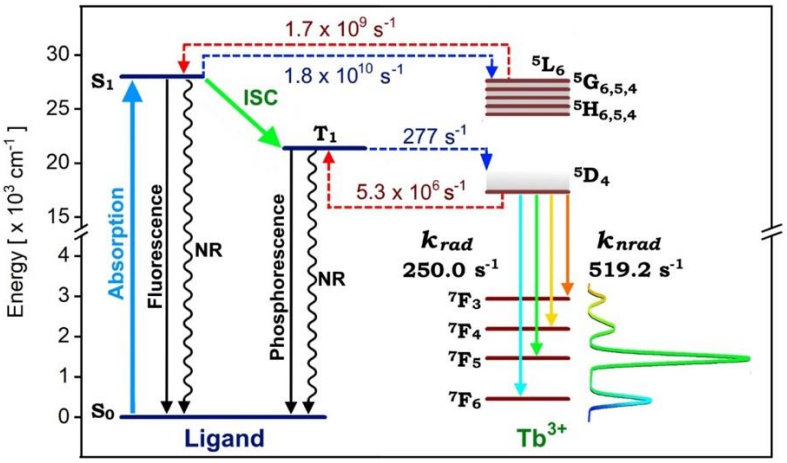

Fig. S69. Jabłoński diagram for Tb(terpy) with energy transfer (red dashed lines and numbers) and back transfer (blue dashed lines and numbers) rates.

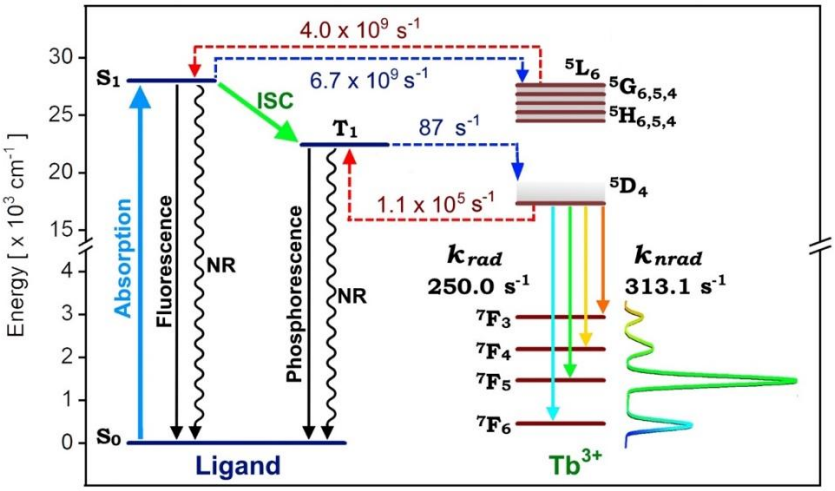

Fig. S70. Jabłoński diagram for Tb(terpyNO_2) with energy transfer (red dashed lines and numbers) and back transfer (blue dashed lines and numbers) rates.

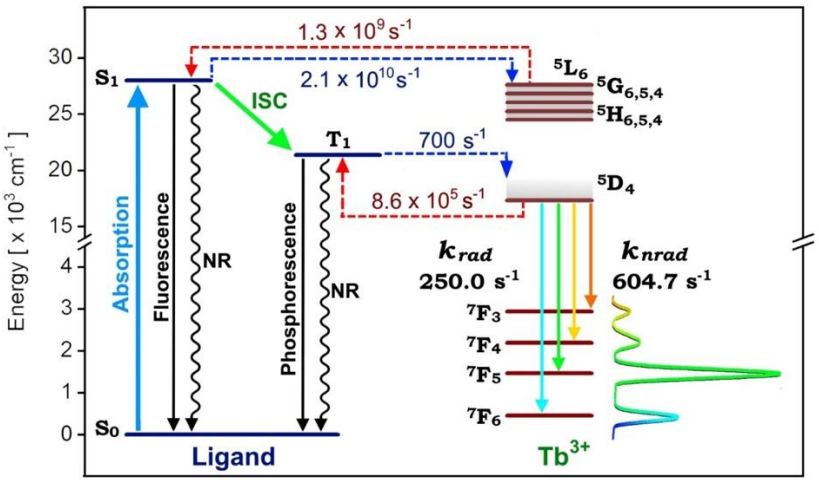

Fig. S71. Jabłoński diagram for Tb(terpyCHO) with energy transfer (red dashed lines and numbers) and back transfer (blue dashed lines and numbers) rates.

Table S1. Forward (W^S) and back (W_b^S) energy transfer rates from ligand's singlet level to Eu(III) and energy forward (W^T) and back (W_b^T) transfer rates from ligand's triplet level to Eu(III). Total energy forward (W^{S+T}) and back (W_b^{S+T}) transfer rates from ligand to Eu(III).

	Eu(terpy)	Eu(terpyNO$_2$)	Eu(terpyBr)	Eu(terpyCHO)
W^S [s^{-1}]	8.18×10^7 (^{5}G$_2$)	7.73×10^6 (^{5}D$_4$)	3.66×10^8 (^{5}G$_2$)	1.38×10^8 (^{5}G$_2$)
(Eu(III) energy level)	4.61×10^6 (^{5}D$_4$)	1.73×10^5 (^{5}G$_6$)	5.22×10^6 (^{5}G$_3$)	3.14×10^6 (^{5}G$_3$)
	1.85×10^6 (^{5}G$_3$)			2.74×10^6 (^{5}D$_4$)
	1.81×10^6 (^{5}G$_6$)			
W_b^S [s^{-1}]	1.06×10^5 (^{5}D$_4$)	2.26×10^5 (^{5}D$_4$)	2.37×10^6 (^{5}G$_2$)	4.94×10^4 (^{5}D$_4$)
(Eu(III) energy level)	2.67×10^4 (^{5}G$_2$)		4.86×10^5 (^{5}D$_4$)	3.54×10^4 (^{5}G$_2$)
			7.35×10^4 (^{5}G$_3$)	1.74×10^3 (^{5}G$_3$)
W^T [s^{-1}]	1.30×10^7 (^{5}D$_2$)	1.56×10^2 (^{5}D$_2$)	4.93×10^7 (^{5}D$_2$)	3.49×10^7 (^{5}D$_2$)
(Eu(III) energy level)			9.97×10^6 (^{5}D$_1$)	
W_b^T [s^{-1}]	2.45×10^5 (^{5}D$_2$)	8.94 (^{5}D$_3$)	8.55×10^6 (^{5}D$_2$)	3.08×10^6 (^{5}D$_2$)
(Eu(III) energy level)		0.12 (^{5}D$_2$)		
W^{S+T} [s^{-1}]	9.09×10^7	7.97×10^6	3.76×10^8	1.45×10^8
W_b^{S+T} [s^{-1}]	1.35×10^5	2.26×10^5	2.94×10^6	8.67×10^4

Table S2. Energy forward (W^S) and back (W_b^S) transfer rates from ligand's singlet level to Tb(III) and energy forward (W^T) and back (W_b^T) transfer rates from ligand's triplet level to Tb(III). Total energy forward (W^{S+T}) and back (W_b^{S+T}) transfer rates from ligand to Tb(III).

	Tb(terpy)	Tb(terpyNO$_2$)	Tb(terpyBr)	Tb(terpyCHO)
W^S [s^{-1}]	1.24×10^{10} ($^5G_6$)	6.31×10^{9} ($^5G_5$)	3.06×10^{10} ($^5G_6$)	1.46×10^{10} ($^5G_6$)
(Tb(III) energy level)	4.60×10^{9} ($^5G_5$)	1.94×10^{8} ($^5L_6$)	1.11×10^{10} ($^5G_5$)	5.52×10^{9} ($^5G_5$)
	5.92×10^{8} ($^5G_4$)	1.73×10^{8} ($^5G_6$)	1.89×10^{9} ($^5G_5$)	8.13×10^{8} ($^5G_4$)
W_b^S [s^{-1}]	1.52×10^{9} ($^5G_6$)	3.92×10^{9} ($^5G_5$)	2.89×10^{9} ($^5G_5$)	7.91×10^{8} ($^5G_5$)
(Tb(III) energy level)	1.60×10^{8} ($^5L_6$)	4.30×10^{7} ($^5L_6$)	3.85×10^{8} ($^5G_6$)	2.15×10^{8} ($^5L_6$)
			2.18×10^{8} ($^5H_5$)	1.59×10^{8} ($^5H_5$)
			2.11×10^{8} ($^5H_4$)	1.20×10^{8} ($^5H_4$)
			1.96×10^{8} ($^5L_6$)	5.52×10^{7} ($^5H_6$)
W^T [s^{-1}]	1.72×10^{2} ($^5G_6$)	86.9 ($^5G_6$)	8.33×10^{4} ($^5D_4$)	4.90×10^{2} ($^5D_4$)
(Tb(III) energy level)	1.05×10^{2} ($^5D_4$)			2.19×10^{2} ($^5D_4$)
W_b^T [s^{-1}]	5.28×10^{6} ($^5G_6$)	1.10×10^{5} ($^5G_6$)	4.11×10^{6} ($^5G_6$)	8.64×10^{5} ($^5G_6$)
(Tb(III) energy level)				
W^{S+T} [s^{-1}]	1.55×10^{10}	6.48×10^{9}	3.09×10^{10}	1.66×10^{10}
W_b^{S+T} [s^{-1}]	1.71×10^{9}	3.95×10^{9}	3.52×10^{9}	1.06×10^{9}

Cartesian coordinates (X, Y, Z in Å) of a DFT optimized structure of Eu-terpyNO_2 complex in its fully bound form

Eu	11.156048	10.686700	10.574480
O	9.627305	14.970018	9.492872
N	9.789592	13.783048	9.589244
O	10.412316	13.248010	10.490319
C	9.175198	12.904084	8.569933
N	9.368874	11.623383	8.765887
C	8.446922	13.472274	7.554383
H	8.338607	14.541883	7.471046
C	7.874140	12.587726	6.656936
H	7.302561	12.955449	5.817337
C	8.031739	11.233237	6.850895
H	7.591627	10.537666	6.152378
C	8.777992	10.770616	7.935826
C	8.935668	9.330060	8.217696
N	9.958266	8.953017	8.997106
C	8.028952	8.419438	7.697569
H	7.193674	8.750103	7.099602
C	8.185632	7.081205	7.989158
H	7.476728	6.353496	7.619998
C	9.260699	6.687181	8.751943
H	9.402807	5.643829	8.987299
C	10.146133	7.647220	9.227959
C	11.355048	7.253283	9.979336
N	12.002095	8.214421	10.647106
C	13.129510	7.903138	11.281035
H	13.629892	8.707199	11.802479
C	13.661553	6.628719	11.295916
H	14.581596	6.434536	11.827702
C	12.995437	5.632935	10.611517

H	13.380244	4.622656	10.585220
C	11.831448	5.949309	9.940632
H	11.318120	5.187350	9.374232
N	11.912882	11.180282	13.407185
O	10.963515	11.797236	12.866649
O	12.516321	10.341282	12.687599
O	12.236683	11.378358	14.556380
N	8.730300	9.867363	12.081706
O	7.758330	9.575797	12.738636
O	8.726574	10.839628	11.282463
O	9.803072	9.216415	12.152164
N	13.181454	10.930362	8.402083
O	12.035764	11.459247	8.349955
O	13.410391	10.204087	9.396416
O	14.004968	11.119408	7.537965
C	14.950860	14.227188	11.338775
H	14.531990	15.219062	11.497869
H	15.527482	13.937744	12.215497
H	15.608551	14.251708	10.471789
C	13.889885	13.280826	11.113457
N	13.045455	12.528620	10.929572

Cartesian coordinates (X, Y, Z in Å) of a DFT optimized structure of Eu-terpyNO_2 complex in its partially unbound form

Eu	11.28625049206846	10.42911692389529	11.46016649550972
O	16.63051904343182	6.87658646827114	14.82354483843591
N	16.16263624974977	6.90338625700979	13.69422914897447
O	16.03348237493207	5.93084963015201	12.97512133205705
C	15.71597741351039	8.23295875459951	13.17853151514228
N	15.23957605321910	8.22424444621027	11.95481989512901
C	15.82799762923555	9.33598363053863	14.01370509832102
H	16.23763015182798	9.24959689891199	15.01396061752124
C	15.38861429963936	10.54803507825154	13.49117122973538
H	15.44548449100414	11.45526610425862	14.08575727902802
C	14.87647260308245	10.58205876976389	12.20036663059646
H	14.54249729332924	11.51865989964037	11.76172053420984
C	14.80677465622720	9.39071639404779	11.46482614432290
C	14.28381313694692	9.39382328398383	10.08003154849495
N	13.29669171174100	10.26690047360205	9.81058873479475
C	14.82728570933241	8.55785430727602	9.10946003233961
H	15.61662804128889	7.86072174638263	9.37376185484655
C	14.34732679259614	8.65563479602103	7.80991734466668
H	14.73615855232118	8.00331300574934	7.03289594470786
C	13.38243925312675	9.60860613138443	7.50799433540436
H	13.00214798907653	9.70794503499785	6.49600495205630
C	12.88145574460265	10.40796307693396	8.53528215139424
C	11.86946393814709	11.45918299074710	8.28892778787866
N	11.12575299052821	11.84101622248367	9.34579929206445
C	10.23798445114507	12.82906397790042	9.19036895421713
H	9.66040796969073	13.10559328078782	10.07104399244736
C	10.03308345928132	13.47273236160937	7.97575997557304
H	9.29717687159633	14.26632144168178	7.89506770694323
C	10.78801087687530	13.07079549929359	6.88069687508011

H	10.65928866278808	13.54552665559082	5.91171334596940
C	11.72375635829585	12.05398186150834	7.03769738758445
H	12.34484599216970	11.74809955040787	6.20096599768822
N	11.71326731958203	12.76004821102396	13.16422184223721
O	10.89693075099423	11.85208520164477	13.49618110967564
O	12.32520283305497	12.57964728392441	12.06145148397506
O	11.90609779982732	13.74481535236643	13.84776200915426
N	8.46484882991834	10.25416158531369	12.07782701988894
O	8.96057340380576	11.14078126773629	11.31089189391824
O	9.28703515508252	9.42082554494469	12.55861573165778
O	7.27727282769548	10.21637406436207	12.32636773252648
N	10.86753544536116	7.96358282462798	9.94992174830181
O	10.31009210543996	9.05261854282196	9.61663749132165
O	11.61976903256960	8.01788460663983	10.97201978366805
O	10.69908679348301	6.93364978425689	9.32836915361526
N	12.19368960060614	9.22183669068975	13.50561959624017
C	12.42455774923805	8.67678661594043	14.50083342661750
C	12.69057605296035	8.00528878858814	15.75006958001671
H	13.34472215707619	8.62477749738293	16.37099007174455
H	13.16933381082732	7.03947026379559	15.56470883500403
H	11.74337707832258	7.84493092059040	16.27431251602714

Cartesian coordinates (X, Y, Z in Å) of a DFT optimized structure of Eu-terpyNO_2 complex in its transit state

Eu	5.33666930212025	12.42898174837353	3.40487504145452
O	5.55134408287196	9.98349289106909	3.26026404552677
O	4.35656410337930	10.85690353543694	1.71250958596920
O	6.60786053547907	14.56675879511654	3.39936912357145
O	5.23585358993578	14.30605064085086	5.02175688142294
N	8.18181828002829	10.43163656267370	1.61545101882722
N	6.19793075398703	12.92557813514006	0.97404218851812
O	4.72870403540328	8.73279462078392	1.70634532002264
O	6.40638390573868	16.11346218624151	4.89000768174190
N	4.87073028437664	9.81667183697478	2.20591843487692
N	6.09645925141899	15.03675628533188	4.45332222920005
C	9.10095040944731	9.93197095642961	2.40163595166477
C	10.17210725498459	10.61393847494537	2.93609950631416
H	10.89925930315595	10.11414948985430	3.55764191343774
C	10.26093153569893	11.96103028653646	2.63085091292231
H	11.07907731757086	12.55449433334856	3.01472639433343
C	9.28567548093739	12.53376266991518	1.83807260490584
H	9.30789162661108	13.58678659034623	1.58995607510811
C	8.26541504746482	11.72938932370253	1.34395558581075
C	7.23834074413247	12.29512362424132	0.42894361273468
C	5.30015081416791	13.50608142637533	0.16075685015353
C	4.18654895971288	14.25120603279067	0.78586725091642
C	7.41108887368165	12.16615229123939	-0.93755081356517
C	5.40672698291319	13.41360993467580	-1.21894385936930
C	3.49206376785728	15.22450278491488	0.08406258584667
N	3.88526760641703	13.97094758882174	2.06325961817578
C	6.46632414143579	12.72495126378763	-1.77346237622953
H	8.27078299693096	11.63504363936790	-1.32260236844787
H	4.65688525714440	13.85626638404910	-1.85752578985020

C	2.46656736990447	15.90906061914311	0.70715194004567
H	3.76277971478844	15.46531081622327	-0.93340426164878
C	2.89184624809210	14.63149053349487	2.65693306616660
H	6.55524196603839	12.63139543209318	-2.84706282111584
C	2.15358314978499	15.60693490282976	2.01760508887356
H	1.92340836793301	16.67566235825680	0.17138557102631
H	2.68152005267646	14.36270316595700	3.68527297568983
H	1.36074829006162	16.11739075821719	2.54437826999454
O	3.13259993112384	12.07137998971803	4.33959864494945
O	4.69530553971941	11.51002299866604	5.69246926923256
O	2.63471860229016	11.31224029289368	6.29718632561916
N	3.46571382898717	11.61638302138963	5.48233819491665
N	8.94087972917367	8.48315026036352	2.73014691042971
O	9.60977978597775	8.05609477404711	3.64686834076004
O	8.16556018080698	7.83356915185393	2.07445801308851
C	9.22348961013545	10.97122683644997	6.32248227918941
H	8.84058827247588	11.00518179829903	7.34121241112649
H	9.46955957001923	9.94139706332229	6.06315483220542
H	10.12086186596242	11.58498508910128	6.25214147967715
C	8.22808822787807	11.46538157922277	5.41295271314882
N	7.43934101316443	11.85593136211764	4.67915741762988